## Plant Ecology & Diversity

# The productivity, metabolism and carbon cycle of two lowland tropical forest plots in south-western Amazonia, Peru

Yadvinder Malhi[a], Filio Farfán Amézquita[b], Christopher E. Doughty[a], Javier E. Silva-Espejo[b], Cécile A.J. Girardin[a], Daniel B. Metcalfe[c], Luiz E.O.C. Aragão[d], Lidia P. Huaraca-Quispe[b], Ivonne Alzamora-Taype[b], Luzmilla Eguiluz-Mora[b], Toby R. Marthews[a], Kate Halladay[a], Carlos A. Quesada[e], Amanda L. Robertson[f], Joshua B. Fisher[g], Joana Zaragoza-Castells[h], Clara M. Rojas-Villagra[b], Yulina Pelaez-Tapia[b], Norma Salinas[ab], Patrick Meir[hi] & Oliver L. Phillips[j]

[a] Environmental Change Institute, School of Geography and the Environment, University of Oxford, Oxford, UK

[b] Universidad Nacional San Antonio Abad del Cusco, Cusco, Peru

[c] Department of Forest Ecology and Management, Swedish University of Agricultural Sciences, Umeå, Sweden

[d] College of Life and Environmental Sciences, University of Exeter, Exeter, UK

[e] Instituto National de Pesquisas da Amazonia (INPA), Manaus, Brazil

[f] University of Alaska, Fairbanks, Alaska, USA

[g] Jet Propulsion Laboratory, Pasadena, California, USA

[h] School of Geosciences, University of Edinburgh, Edinburgh, UK

[i] Research School of Biology, Australian National University, Canberra, Australia

[j] Department of Geography, University of Leeds, Leeds, UK
Published online: 16 Sep 2013.

PLEASE SCROLL DOWN FOR ARTICLE

Taylor & Francis
Taylor & Francis Group

# The productivity, metabolism and carbon cycle of two lowland tropical forest plots in south-western Amazonia, Peru

Yadvinder Malhi[a]*, Filio Farfán Amézquita[b], Christopher E. Doughty[a], Javier E. Silva-Espejo[b], Cécile A.J. Girardin[a], Daniel B. Metcalfe[c], Luiz E.O.C. Aragão[d], Lidia P. Huaraca-Quispe[b], Ivonne Alzamora-Taype[b], Luzmilla Eguiluz-Mora[b], Toby R. Marthews[a], Kate Halladay[a], Carlos A. Quesada[e], Amanda L. Robertson[f], Joshua B. Fisher[g], Joana Zaragoza-Castells[h], Clara M. Rojas-Villagra[b], Yulina Pelaez-Tapia[b], Norma Salinas[a,b], Patrick Meir[h,i] and Oliver L. Phillips[j]

[a]*Environmental Change Institute, School of Geography and the Environment, University of Oxford, Oxford, UK;* [b]*Universidad Nacional San Antonio Abad del Cusco, Cusco, Peru;* [c]*Department of Forest Ecology and Management, Swedish University of Agricultural Sciences, Umeå, Sweden;* [d]*College of Life and Environmental Sciences, University of Exeter, Exeter, UK;* [e]*Instituto National de Pesquisas da Amazonia (INPA), Manaus, Brazil;* [f]*University of Alaska, Fairbanks, Alaska, USA;* [g]*Jet Propulsion Laboratory, Pasadena, California, USA;* [h]*School of Geosciences, University of Edinburgh, Edinburgh, UK;* [i]*Research School of Biology, Australian National University, Canberra, Australia;* [j]*Department of Geography, University of Leeds, Leeds, UK*

**Background:** The forests of western Amazonia are known to be more dynamic that the better-studied forests of eastern Amazonia, but there has been no comprehensive description of the carbon cycle of a western Amazonian forest.

**Aims:** We present the carbon budget of two forest plots in Tambopata in south-eastern Peru, western Amazonia. In particular, we present, for the first time, the seasonal variation in the detailed carbon budget of a tropical forest.

**Methods:** We measured the major components of net primary production (NPP) and total autotrophic respiration over 3–6 years.

**Results:** The NPP for the two plots was $15.1 \pm 0.8$ and $14.2 \pm 1.0$ Mg C ha$^{-1}$ year$^{-1}$, the gross primary productivity (GPP) was $35.5 \pm 3.6$ and $34.5 \pm 3.5$ Mg C ha$^{-1}$ year$^{-1}$, and the carbon use efficiency (CUE) was $0.42 \pm 0.05$ and $0.41 \pm 0.05$. NPP and CUE showed a large degree of seasonality.

**Conclusions:** The two plots were similar in carbon cycling characteristics despite the different soils, the most notable difference being high allocation of NPP to canopy and low allocation to fine roots in the Holocene floodplain plot. The timing of the minima in the wet–dry transition suggests they are driven by phenological rhythms rather than being driven directly by water stress. When compared with results from forests on infertile forests in humid lowland eastern Amazonia, the plots have slightly higher GPP, but similar patterns of CUE and carbon allocation.

**Keywords:** allocation; GPP; herbivory; NPP; phenology; seasonality; soil respiration; stem respiration; tropical forests; western Amazonia

## Introduction

Tropical forests and savannas account for over 60% of global terrestrial photosynthesis, and play a significant role in the global carbon cycle through the fixation, respiration and cycling of carbon. Hence a mechanistic understanding of the patterns and processes underlying the productivity and carbon cycle of tropical forests is very valuable. Many studies of tropical forest carbon cycling have focussed on a single aspect of the carbon budget, most often above-ground wood productivity (e.g. Malhi et al. 2004) and litterfall (e.g. Chave et al. 2010), the most easily estimated components, or at the other extreme canopy photosynthesis (gross primary productivity, GPP) as estimated through above-canopy $CO_2$ fluxes (e.g. Malhi 2012). However, the above-ground wood and canopy production components make up only a small fraction of the total carbon uptake (or GPP) of a forest (Malhi et al. 2009). Recently a more comprehensive approach that attempts to quantify all the main components of productivity and respiration has gained prominence (Chambers et al. 2004; Cavaleri et al. 2006; Malhi et al. 2009; Metcalfe et al. 2010; Tan et al. 2010; Malhi 2012). This approach was first established by the pioneers of tropical ecosystem ecology (e.g. Odum and Pigeon 1970 in Puerto Rico; Kira 1978 in Malaysia), but has recently attracted new interest in the context of new and more accurate $CO_2$ flux measurement technology, and the advent of standardised multi-site measurements across tropical regions.

Amazonia is the greatest of the world's tropical forest regions, accounting for approximately one-half of global tropical forest area. Its ecosystem science has probably received more scientific attention that other tropical forest regions, particularly in the context of the Large Scale Biosphere-Atmosphere programme in Brazil from the mid-1990s onwards. However, the vast majority of this research effort has focussed on Brazil, and predominantly on highly infertile soils, characteristic of much of lowland Brazilian Amazonia (Quesada et al. 2010). The western part of

lowland Amazonia, however, has very different ecological and soil conditions. This is as a result of its particular geological history, once being a lake or inland sea, and subsequent gentle erosional uplift associated with the rise of the Andes, resulting in both the exposure of old, more fertile sediments (Higgins et al. 2011) and also the deposition of fertile alluvial terraces in the meander belts of rivers carrying nutrient-rich sediments from their origins in the Andes (Hoorn et al. 2010). Forest plot inventory studies have noted that western Amazonian forests, when compared with typical forests from eastern Amazonia, tend to have higher wood productivity (Malhi et al. 2004), higher turnover (Phillips et al. 2004) and different species composition (ter Steege et al. 2006) with lower wood density (Baker et al. 2004). Recently, we documented that sites in western Amazonia appeared to have higher total net primary productivity (NPP) (canopy litterfall plus wood production plus root production) than sites in the eastern Amazon (Aragão et al. 2009), with higher availability of phosphorus in particular being a likely underlying cause of this difference (Quesada et al. 2012).

However, to date the only comprehensive studies of the carbon cycle of tropical forests have been restricted to sites in central and eastern Amazonia (Chambers et al. 2004; Malhi et al. 2009; Metcalfe et al. 2010). Here, we report the first such study in western Amazonia. We present data from two 1 ha plots in the lowland Amazonian forests of south-eastern Peru. We focus here on the carbon budget and seasonal variation of the carbon cycle of these plots. In future papers we will explore further the inter-annual variability of the carbon cycle and make more extensive multiple-site comparisons.

We asked the following specific questions:

(1) How do the components of NPP vary over the seasonal cycle in these two plots, and how do they relate to climate conditions?
(2) How do the components of autotrophic and heterotrophic respiration vary over the seasonal cycle in these two plots, and how do they relate to climate conditions?
(3) How does the total cycle of carbon production, carbon-use efficiency (the ratio of NPP to GPP) and NPP allocation differ between the plots, and compare with previously published results from Brazilian Amazonia?

## Materials and methods

### Site characteristics

The two study plots were located in the Tambopata-Candamo Reserve, in the Madre de Dios region of Peru, based on long-term 1 ha forest inventory plots that were established in the early 1980s (Gentry 1988), and have been re-censused multiple times and are now part of the RAINFOR forest inventory network (Malhi et al. 2002). Permanent plots at Tambopata have been intensively

studied, with soils, diversity, composition, leaf nutrition, biomass, biomass change, fruit production, and forest dynamics all reported elsewhere (e.g. Gentry 1988; Phillips 1993; Phillips et al. 1998, 2004, 2009; Baker et al. 2004; Quesada et al. 2010, 2011). Two of these plots, TAM-05 (12° 49′ 49.04″ S, 69° 16′ 13.92″ W) and TAM-06 (12° 49′ 49.04″ S, 69° 16′ 13.92″ W), are the focus of the present paper. Partial data on forest carbon cycling have previously been published for these plots, notably on soil carbon cycling by Zimmermann et al. (2009, 2010), woody productivity in Malhi et al. (2004), coarse woody debris production and decay in Baker et al. (2007), forest above-ground productivity in Aragão et al. (2009), ecosystem modelling in Marthews et al. (2012), stem respiration in Robertson et al. (2010), landscape context in Anderson et al. (2009) and root dynamics in Girardin et al. (2013). Here we provide the first comprehensive description (and an extended time series) of the carbon cycling at these Tambopata plots.

Despite the relative proximity of the plots, the soils at TAM-05 and TAM-06 differ both in terms of geological history and fertility (Table 1). The geomorphology of the study region is based on old floodplains of the meandering Tambopata River. The region is slowly rising in elevation because of uplift associated with the Andes, leaving old floodplains as raised terraces. TAM-05 is situated on a Pleistocene terrace (<100,000 years old), while TAM-06 is situated on a recent Holocene floodplain terrace (<10,000 years old; with part of the plot still occasionally inundated under extreme high water conditions a few

Table 1. Average (0–30cm) soil data for TAM-05 and TAM-06 plots, Tambopata, Madre de Dios, Peru, extracted from Quesada et al. (2010). $P_{ex}$, extractable pool (total minus residual) or biologically active P; $P_a$, readily available pool; $P_{Total}$, total soil phosphorus pool (all in mg kg$^{-1}$); $\Sigma_{RB}$, total reserve bases; $Ca_{ex}$, $Mg_{ex}$, $K_{ex}$, $Al_{ex}$ – exchangeable calcium, magnesium, potassium and aluminium concentrations; $\Sigma_B$, sum of exchangeable bases; $I_E$, effective soil cation exchange capacity (all in mmol$_c$ kg$^{-1}$). Particle size is shown in fractions; total nitrogen and carbon are in %.

| PLOT | TAM-05 | TAM-06 |
|---|---|---|
| pH | 3.91 | 5.06 |
| N | 0.16 | 0.17 |
| C | 1.51 | 1.20 |
| C:N | 9.37 | 7.05 |
| $P_a$ | 32.34 | 33.06 |
| $P_{ex}$ | 77.32 | 214.57 |
| $P_{Total}$ | 256.29 | 528.80 |
| $\Sigma_{RB}$ | 272.75 | 978.28 |
| $Ca_{ex}$ | 0.30 | 26.80 |
| $Mg_{ex}$ | 1.00 | 21.60 |
| $K_{ex}$ | 0.90 | 1.50 |
| $Na_{ex}$ | 0.10 | 0.20 |
| $Al_{ex}$ | 42.50 | 6.70 |
| $\Sigma_B$ | 2.30 | 50.10 |
| $I_{ex}$ | 44.80 | 56.80 |
| Sand | 0.40 | 0.02 |
| Clay | 0.44 | 0.46 |
| Silt | 0.17 | 0.52 |

days per year). Detailed soil data for TAM-05 and TAM-06 are summarised in Table 1. The age difference between the plots is reflected in their contrasting total reserve base content ($\Sigma_{RB}$; 273 and 978 mmol$_c$ kg$^{-1}$ for TAM-05 and TAM-06, respectively; Table 1), a chemical weathering index which takes in account the total concentration of soil cations (Ca, Mg, K, Na), and is thought to represent the abundance of easily weatherable minerals (Delvaux et al. 1989). Higher $\Sigma_{RB}$ values suggest younger, less weathered soils, while lower values are an indication of more weathering.

The soil at TAM-06 also has a larger phosphorus pool (256 and 529 mg kg$^{-1}$ for TAM-05 and TAM-06, respectively), a relatively high value for an Amazonian soil (Quesada et al. 2010). The partitioning of P in different fractions indicates that immediately available P pools ($P_a$) are quite similar between the plots, and thus most of the difference in total P content can be explained by P located in slow turnover pools and residual fractions. These slow turnover P pools are of importance for nutrient cycling in the region and have been shown to be important correlates of forest productivity in Amazonia (Quesada et al. 2011, 2012), probably by buffering the uptake of more labile forms of P. TAM-05 has high sand content (40%) whereas TAM-06 is predominantly clay and silt (sand content 2%). The soil at TAM-05 was classified as a Haplic cambisol (IUSS Working Group WRB 2006), and that at TAM-06 is a Haplic alisol (Table 1; Quesada et al. 2010). No soil hardpan layers prevent root penetration through the soil profile, but roots were virtually absent in soil layers >100 cm deep (Quesada et al. 2011). A map of the plots and site is given in Anderson et al. (2010).

Canopy leaf nutrient data from Lloyd et al. (2010) indicated similar levels of average leaf N between the two plots (24.0 mg g$^{-1}$ for TAM-05 and 24.8 mg g$^{-1}$ for TAM-06) but higher average concentrations of leaf P in TAM-06 (1.05 mg g$^{-1}$ and 1.88 mg g$^{-1}$ for TAM-05 and TAM-06), consistent with the soil nutrient patterns. Leaf level P has been suggested to be a strong determinant of canopy photosynthesis in Amazonian forests (Domingues et al. 2010; Mercado et al. 2011), suggesting that TAM-06 would be more fertile and have higher GPP than TAM-05.

The vegetation is closed canopy forest with a similar mean (± s.e.) canopy height on both plots (estimated as height of trees ≥ 40 cm diameter at breast height (DBH), 25 ± 8 m for TAM-05, and 27 ± 8 m for TAM-06) and high plant species diversity. TAM-06 is particularly abundant in palms of the species *Socratea exorrhiza* and *Iriartea deltoidea*, which together constitute over 30% of the stems ≥ 10 cm DBH in the plot.

### Measurements

The intensive monitoring study was established in January 2005, and was expanded in scope of measurements in 2009. In the main text we present only a concise description and summary tables of methods (Tables 2 and 3). These

are elaborated further in the online supplemental material. The protocols used are based on those developed by the RAINFOR-GEM network, and are explained in detailed in the RAINFOR-GEM manual (http://gem.tropicalforests.ox.ac.uk).

### Meteorological data

Solar radiation, air temperature, relative humidity and precipitation time series were collected from an automatic weather station (AWS) in a clearing at the Explorers' Inn lodge about 500 m from TAM-06 (12.836° S, 69.294° W). These data were quality controlled to remove outliers and then gap-filled, as explained in the Supplementary Material, based on regression against a nearby weather station at Puerto Maldonado, or for precipitation from the nearest grid point of the Tropical Rainfall Measuring Mission 3B43 product, calibrated to the AWS.

Soil moisture (0–30 cm depth) was measured at the 25 soil respiration points in each plot on a monthly basis, using a Hydrosense probe (Campbell Scientific Ltd, Loughborough, UK). The maximum climatological water deficit (MCWD), a climatological measure of tropical forest water stress, was calculated by using the gap-filled monthly time series for precipitation according to the equations listed in Aragão et al. (2009).

### Net primary productivity

All major biomass production components of NPP components were measured for this study. We do not measure the components of NPP not associated with plant biomass production (e.g. volatile organics production, root exudates and export to root symbionts – the later two are probably incorporated in our rhizosphere respiration term). Vicca et al. (2012) suggested the term biomass production (BP) for the biomass components of NPP, and the term biomass production efficiency (BPE) as the ratio of BP to GPP. However, to retain consistency with the terminology of the wider NPP literature here we implicitly assume that BP is close to total actual NPP, and retain the terminology NPP for the sum of the biomass production components, and carbon use efficiency (CUE) for the ratio NPP/GPP.

The protocols used to estimate ecosystem C flux components are those developed by the Global Ecosystems Monitoring (GEM) network. A detailed description of the measurement protocols is available online for download at the GEM website (http://gem.tropicalforests.ox.ac.uk) and in the online supplemental material accompanying this paper. Summaries of the different components quantified, and the field methods and data processing techniques used are presented in Tables 2 and 3, respectively.

Measured above-ground net primary productivity ($NPP_{AG}$) components included:

(a) Above-ground coarse wood net primary productivity ($NPP_{ACW}$), estimated from annual tree census of all trees ≥ 10 cm DBH, and sub-plots of trees

Table 2.  Methods for intensive monitoring of carbon dynamics at the Tambopata plots in Madre de Dios, Peru (also see online supplemental material and RAINFOR-GEM manual 2012).

| | Component | Description | Sampling period | Sampling interval |
|---|---|---|---|---|
| **Above-ground net primary productivity ($NPP_{AG}$)** | Above-ground coarse wood net primary productivity ($NPP_{ACW}$) | Forest inventory: All trees $\geq$ 10 cm DBH censused to determine growth rate of existing surviving trees and rate of recruitment of new trees. Stem biomass calculated using the Chave et al. (2005) allometric equation for tropical wet forests, employing diameter, height and wood density data. Four 15 m $\times$ 15 m and one 20 m $\times$ 20 m subplots established to census small trees (2.5–10 cm DBH) | 2005–2011 | Every year (trees $\geq$ 10 cm DBH) Every 6 months (trees 2.5–10 cm DBH) |
| | | Seasonal growth: Dendrometers installed on all trees ($\geq$ 10 cm DBH) in each plot to determine variation in growth rates with higher precision. | 2005–2011 | Every 3 months |
| | Branch turnover net primary productivity ($NPP_{branch\ turnover}$) | Branches > 2 cm diameter (excluding those fallen from dead trees) were surveyed within four 1 m $\times$ 100 m transects; small branches were cut to include only the transect-crossing component, removed and weighed. Larger branches had their dimensions taken (diameter at 3 points) and all were assigned a wood density value according to their decomposition class. | 2009–2011 | Every 3 months |
| | Litterfall net primary productivity ($NPP_{litterfall}$) | Collected in 0.25 m$^2$ (50 cm $\times$ 50 cm) litter traps placed at 1 m above the ground at the centre of each of the 25 subplots in each plot. Litter is separated into its components, oven dried at 80 °C to constant mass and weighed. | Feb 2005–Mar 2011 | Every 14 days |
| | Leaf Area Index (LAI) | Canopy images recorded with a digital camera and hemispherical lens near the centre of each of the 25 subplots, at a standard height of 1 m, and during overcast conditions. LAI estimated from these images using CAN-EYE software. | Jan 2005–Aug 2010 | Every month |
| | Loss to leaf herbivory ($NPP_{herbivory}$) | Leaves collected in the 25 litterfall traps in each plot were photographed prior to being dried. Leaves were scanned to calculate the area of each individual leaf lost to herbivory. | 2009–2011 | Every 2 months |
| **Belowground net primary productivity ($NPP_{BG}$)** | Coarse root net primary productivity ($NPP_{coarse\ root}$) | Not measured directly. Estimated as 0.21 $\pm$ 0.03 of above-ground woody productivity. | .n/a | Not directly measured |
| | Fine root net primary productivity ($NPP_{fine\ root}$) | Sixteen ingrowth cores (mesh cages 12 cm diameter, installed to 30 cm depth) were installed in each plot. Cores were extracted and roots were manually removed from the soil samples in four 10 min time steps and the pattern of cumulative extraction over time was used to predict root extraction beyond 40 min. Root-free soil was then re-inserted into the ingrowth core. Collected roots were thoroughly rinsed, oven dried at 80 °C to constant mass, and weighed. | Sep 2009–Mar 2011 | Every 3 months |

(*Continued*)

Table 2.    (*Continued*)

| | Component | Description | Sampling period | Sampling interval |
|---|---|---|---|---|
| **Autotrophic and heterotrophic respiration ($R_a$ and $R_h$)** | Total Soil $CO_2$ efflux | Total soil $CO_2$ efflux was measured using a closed dynamic chamber method with an infra-red gas analyser and soil respiration chamber (EGM-4 IRGA and SRC-1 chamber, PP Systems, Hitchin, UK) sealed to a permanent collar in the soil. | 2005–2011 | Every month |
| | Soil $CO_2$ efflux partitioned into autotrophic and heterotrophic components | At four points at each corner of the plot, we placed plastic tubes of 12 cm diameter; three tubes with short collars (10 cm depth) allowing both heterotrophic and rhizosphere respiration, three tubes with longer collars (40 cm depth) with no windows to exclude both roots and mycorrhizae. At the centre of each plot, a control experiment was carried out in order to assess the effects of root severing and soil structure disturbance that occurs during installation. | Feb 2009–Jun 2011 | Every month |
| | Canopy respiration | Leaf gas exchange measurements of $R_{dark}$ were performed using infra-red gas analysers. To obtain the leaves, branches of sun-lit, canopy-top foliage were detached and immediately re-cut under water to restore hydraulic connectivity for subsequent gas exchange measurement. The leaves were fully darkened for 30 min prior to measuring $R_{dark}$. | May 2007 (wet season – 50 trees) and July 2010 (dry season- 156 trees) | Once in dry season, once in wet season |
| | Aboveground live wood respiration | Bole respiration was measured using a closed dynamic chamber method, from 25 trees distributed evenly throughout each plot at 1.3 m height with an IRGA (EGM-4) and soil respiration chamber (SRC-1) connected to a permanent collar, sealed to the tree bole surface. | Mar 2006–Dec 2010 | Every month |
| | Coarse root respiration | This component of respiration was not measured directly but estimated by multiplying above-ground live wood respiration by 0.21. This respiration is assumed to be very close to the trunk and missed by soil respiration chambers. | n/a | Not directly measured |

$\geq 2.5$ cm DBH. Seasonal variation was estimated from dendrometer bands attached to almost all trees.

(b) Branch turnover net primary productivity ($NPP_{branch\ turnover}$), estimated by setting up four 1 m × 100 m transects, where woody material ($\geq 2$ cm diameter) fresh-fallen from live trees was collected every 3 months. The turnover of branches, where trees shed branches and grow new ones, can generate a significant component of woody NPP that is not accounted for by the static tree allometries used above.

(c) Annual values of litterfall net primary productivity ($NPP_{litterfall}$), estimated from bi-weekly litter collections from 25 litter traps. $NPP_{litterfall}$ was further partitioned into twigs, flowers, fruit, bromeliads,

other epiphytes (Table 4) and unidentified material (not shown). Seasonal variations in leaf NPP were calculated by combining leaf litterfall data with canopy leaf area index estimates, which were derived from monthly hemispherical photographs of the canopy.

(d) Loss to leaf herbivory ($NPP_{herbivory}$), the fraction of $NPP_{canopy}$ lost to herbivory prior to litterfall, estimated by calculating leaf area lost in scanned litterfall samples.

(e) Palm leaf and fruit productivity, treated separately because of the large size of palm leaves and the clustered nature of palm fruit drop.

Below-ground net primary productivity ($NPP_{BG}$) components consisted of fine and coarse roots $NPP$:

Table 3.   Data analysis for intensive monitoring of carbon dynamics at the forest plots in Tambopata, Peru.

| | Component | Data processing details |
|---|---|---|
| **Above-ground net primary productivity (*NPP$_{AG}$*)** | Above-ground coarse wood net primary productivity (*NPP$_{ACW}$*) | Biomass calculated using the Chave et al. (2005) allometric equation for tropical moist forests: AGB = 0.0776 × ($\rho$ DBH$^2$ H)$^{0.94}$, where AGB is aboveground biomass (kg), $\rho$ is density of wood (g cm$^{-3}$), $D$ is DBH (cm), and $H$ is height (m). To convert biomass values into carbon, we assumed that dry stem biomass is 47.3% carbon (Martin and Thomas 2011). For the few trees where height data were not available, it was estimated from the Feldpausch et al. (2011) allometric equation. |
| | *NPP*$_{branch\ turnover}$ | See RAINFOR-GEM manual (2012, p.61) for description of decomposition status and surface area formulas. |
| | Litterfall net primary productivity (*NPP*$_{litterfall}$) | Litter is estimated to be 49.2% carbon, based on values measured for leaves in Tambopata (S. Patiño, unpublished analysis). |
| | Leaf area index (LAI) | LAI estimated using "true PAI" output from the CANEYE program which accounts for clumping of foliage, and assuming a fixed leaf inclination angle of 42.5°. Leaves were separated into sunlit and shaded fractions using the following equation: $F_{sunlit} = (1 − \exp(−K*LAI))/K$ where $K$ is the light extinction coefficient, and $F_{sunlit}$ is the sunlit leaf fraction (Doughty and Goulden 2008). The model assumptions are randomly distributed leaves, and K = 0.5/cos(Z), where Z is the solar zenith angle, which was set to 30°. |
| | Loss to leaf herbivory | The fractional herbivory ($H$) for each leaf was calculated as: $H = (A_{nh} − A_h) / A_{nh}$, where $A_h$ is the area of each individual leaf including the damage incurred by herbivory and $A_{nh}$ is the leaf area prior to herbivory. The mean values of $H$ were calculated across all leaves collected both per litterfall trap and per plot. |
| **Belowground net primary productivity (*NPP$_{BG}$*)** | *NPP*$_{coarse\ root}$ | Estimated as a fixed proportion (0.21 ± 0.03) of above-ground woody NPP (*NPP*$_{ACW}$ + *NPP*$_{branch\ turnover}$). |
| | Fine root net primary productivity (*NPP*$_{fine\ root}$) | Typically there was an additional 34% correction factor for fine roots not collected within 40 min. A further correction (of 39%) was applied for unmeasured roots below 30 cm depth according to fine root biomass profiles. |
| **Autotrophic (*R$_a$*) and heterotrophic (*R$_h$*) respiration** | Total soil CO$_2$ efflux | Soil surface temperature (T260 probe, Testo Ltd., Hampshire, UK) and moisture (Hydrosense probe, Campbell Scientific Ltd., Loughborough, UK) were recorded at each point after efflux measurement. |
| | Soil CO$_2$ efflux (autotrophic and heterotrophic) | The partitioning experiment allows estimation of the relative contributions of surface organic litter, rhizosphere and soil organic matter to total soil CO$_2$ efflux. Contributions are estimated from differences between collars subjected to different treatments, in excess of pre-existing spatial variation. To allow for possible systematic biases, we assigned a 10% systematic uncertainty to the partitioning results, in addition to the sampling uncertainty. |
| | Canopy respiration | To scale to whole-canopy respiration, mean dark respiration for shade and sunlit leaves were multiplied by the respective estimated fractions of total LAI. The wet season respiration mean was applied to all months with > 100 mm rain; the dry season months, measured dry season respiration was linearly scaled by the soil moisture saturation to allow for more continuous variation of leaf respiration. To account for daytime light inhibition of leaf dark respiration, we apply an inhibition factor: 67% of daytime leaf dark respiration, 34% of total leaf dark respiration (Malhi et al. 2009). These were calculated by applying the Atkin et al. (2000) equations for light inhibition of leaf respiration to a plot in Tapajós forest in Brazil (Malhi et al. 2009; Lloyd et al. 2010). |
| | Above-ground live wood respiration (*R$_{stem}$*) | To estimate plot-level stem respiration tree respiration per unit bole area was multiplied by bole surface area (SA) for each tree, estimated with the following equation (Chambers et al. 2004): $\log_{10}(SA) = −0.105 − 0.686 \log(DBH) + 2.208 \log(DBH)^2 − 0.627 \log(DBH)$, where H is tree height, and DBH is bole diameter at 1.3 m height. Finally, for all 25 trees together we regressed mean annual bole respiration against total annual growth. To allow for considerable possible systematic biases in this scaling, we assigned a systematic uncertainty of 30% to the estimated total live woody respiration. |
| | Coarse root respiration | In recognition of the substantial uncertainty in this estimate, we assigned a 50% error to the multiplying factor. |

Table 4. Components of NPP, respiration and total carbon budget for the two plots at Tambopata. All units are Mg C ha$^{-1}$ year$^{-1}$, excepted CUE, which is dimensionless.

| Plot | Tambopata 05 | | | Tambopata 06 | | |
|---|---|---|---|---|---|---|
| | Mean | Sample error | Total error | Mean | Sample error | Total error |
| $NPP_{litterfall}$ | 5.39 | 0.35 | 0.35 | 4.94 | 0.40 | 0.40 |
| $NPP_{leaf}$ | 4.03 | 0.27 | 0.27 | 3.71 | 0.39 | 0.39 |
| $NPP_{flower}$ | 0.16 | 0.05 | 0.05 | 0.15 | 0.05 | 0.05 |
| $NPP_{fruit}$ | 0.26 | 0.07 | 0.07 | 0.40 | 0.14 | 0.14 |
| $NPP_{twigs}$ | 0.86 | 0.18 | 0.18 | 0.72 | 0.17 | 0.17 |
| $NPP_{herbivory}$ | 0.76 | 0.05 | 0.05 | 0.70 | 0.07 | 0.07 |
| $NPP_{palm}$ | 0.22 | 0.07 | 0.07 | 2.81 | 0.84 | 0.84 |
| $NPP_{branch turnover}$ | 0.95 | 0.10 | 0.10 | 0.50 | 0.05 | 0.05 |
| $NPP_{stems>10 cm dbh}$ | 2.41 | 0.24 | 0.24 | 2.49 | 0.25 | 0.25 |
| $NPP_{stems<10 cm dbh}$ | 0.23 | 0.02 | 0.02 | 0.15 | 0.01 | 0.01 |
| $NPP_{coarse root}$ | 0.51 | 0.05 | 0.05 | 0.52 | 0.05 | 0.05 |
| $NPP_{fine root}$ | 4.54 | 0.71 | 0.71 | 2.11 | 0.31 | 0.31 |
| $R_{leaf}$ | 8.86 | 1.01 | 2.84 | 6.43 | 0.76 | 2.07 |
| $R_{stem}$ | 5.43 | 0.69 | 1.77 | 7.62 | 0.96 | 2.48 |
| $R_{rhizosphere}$ | 5.07 | 0.35 | 0.61 | 4.62 | 0.34 | 0.57 |
| $R_{coarseroot}$ | 1.14 | 0.00 | 0.59 | 1.60 | 0.00 | 0.82 |
| $R_{soilhet}$ | 7.08 | 0.49 | 0.86 | 6.34 | 0.43 | 0.76 |
| $R_{soil}$ | 12.15 | 0.60 | 0.60 | 10.97 | 0.54 | 0.54 |
| $R_a$ | 20.46 | 1.28 | 3.45 | 20.26 | 1.29 | 3.38 |
| NPP | 15.01 | 0.84 | 0.84 | 14.21 | 1.02 | 1.02 |
| GPP | 35.47 | 1.53 | 3.55 | 34.47 | 1.64 | 3.53 |
| CUE | 0.42 | 0.03 | 0.05 | 0.41 | 0.04 | 0.05 |

(f) Coarse root productivity ($NPP_{coarse root}$) is extremely difficult to directly sample without damaging trees, and was estimated as $0.21 \pm 0.03$ of above-ground woody productivity (as in Malhi et al. 2009).

(g) Fine root net primary productivity ($NPP_{fine root}$) was quantified using 3-monthly collections of 16 ingrowth cores, with corrections applied for deep fine roots and undersampling of very fine roots.

*Autotrophic and heterotrophic respiration*

We quantified the major autotrophic and heterotrophic fluxes of $CO_2$.

(h) Total soil $CO_2$ efflux and its partition into heterotrophic and autotrophic components. We measured total soil $CO_2$ efflux every month at the same point in each of the 25 sub-plots on each plot. The autotrophic and heterotrophic components of soil respiration were quantified using a partitioning experiment similar to that described in Metcalfe et al. (2007) (Table 2 and supplemental material).

(i) Above-ground live wood respiration, $R_{stem}$, was quantified at monthly intervals by measuring rates of CO2 accumulation to chambers attached to the tree trunk, and scaling using stem surface area allometries.

(j) Canopy leaf dark respiration, $R_{leaf}$. This was estimated by measuring dark respiration of canopy

Table 5. Leaf dark respiration values, separated by season and by sun/shade position at the Tambopata plots in the dry season (July 2010; $n = 76/80$ for TAM-05/TAM-06) and wet season (May 2007; $n = 25/25$ for TAM-05/TAM-06). Units are μmol $CO_2$ m$^{-2}$ s$^{-1}$. Significant difference between plots is denoted by: *$P < 0.05$; **$P < 0.01$.

| | Dry sun | Dry shade | Wet sun | Wet shade |
|---|---|---|---|---|
| TAM-05 | $0.64 \pm 0.07$ | Not collected | $0.67 \pm 0.08$* | $0.79 \pm 0.09$** |
| TAM-06 | $0.57 \pm 0.07$ | $0.43 \pm 0.02$ | $0.49 \pm 0.07$* | $0.56 \pm 0.06$** |

leaves in dry season and wet season campaigns, applying a correction for daytime light inhibition of leaf dark respiration and scaling by leaf area index.

(k) Coarse root respiration. A substantial amount of wood respiration may occur in or near the root core immediately below the bole, but this has rarely been measured and is not included in our soil respiration partitioning methodology. In addition, even small coarse roots are too slow-growing to be present in 3-monthly ingrowth cores. We therefore estimate this term separately. Coarse root respiration was estimated by multiplying estimated above-ground live wood respiration by $0.21 \pm 0.10$, the same ratio used in this study to estimate coarse root biomass and growth based on published values (Jackson et al. 1996; Cairns et al. 1997). In recognition of the substantial uncertainty in this estimate, we assigned a 50% error ($\pm 0.10$) to the multiplying factor (Table 4).

*Calculation of net primary productivity, gross primary productivity and carbon use efficiency*

Above- and below-round net primary productivity, $NPP_{AG}$ and $NPP_{BG}$ were calculated as the sum of the measured components:

$$NPP_{AG} = NPP_{ACW \geq 10 cm} + NPP_{ACW < 10 cm} + NPP_{litterfall}$$
$$+ NPP_{branch turnover} + NPP_{herbivory} + NPP_{palm}$$
(1)

$$NPP_{BG} = NPP_{fine root} + NPP_{coarse root} \qquad (2)$$

Total autotrophic respiration was estimated as

$$R_a = R_{leaf} + R_{stem} + R_{rhizosphere} + R_{coarse root} \qquad (3)$$

The above-ground NPP calculation neglects several small NPP terms, such NPP lost as volatile organic emissions, non-measured litter trapped in the canopy, or dropped from ground flora below the litter traps. Malhi et al. (2009) showed that $NPP_{VOC}$ is a small component of the carbon budget in a central Amazonian forest ($0.1 \pm 0.05$ Mg C ha$^{-1}$ year$^{-1}$), and that near-closure of

the carbon budget for several sites in Brazil suggests that the other neglected NPP terms are relatively minor. For below-ground NPP, the allocation to root exudates and to mycorrhizae is neglected. In effect we treat root exudation and transfer to mycorrhizae as rhizosphere autotrophic respiration rather than as NPP. This issue in the context of our Amazonian measurements will be explored in a future paper.

In plant-level steady state conditions (and on annual timescales or longer where there is little net non-structural carbohydrate storage), GPP, the carbon taken up via photosynthesis, should be approximately equal to the plant carbon expenditure (PCE), the amount of carbon used for NPP and autotrophic plant respiration ($R_a$). Hence, we estimated GPP as:

$$GPP = PCE = NPP_{Total} + R_a \qquad (4)$$

(i.e. GPP = plant carbon expenditure PCE, Metcalfe et al. 2010). On a seasonal timescale, PCE may not be equivalent to GPP if there is a substantial seasonal cycle of storage of non-structural carbohydrates (e.g. if products of "excess" GPP are stored in one season and allocated to NPP or metabolism in another season).

Using these data, we estimated the CUE as the proportion of total GPP invested in $NPP_{Total}$ rather than $R_a$:

$$CUE = NPP_{Total}/GPP = NPP_{Total}/(NPP_{Total} + R_a) \quad (5)$$

### Statistics and error analysis

The data were used to describe the spatial and temporal variations of above- and below-ground carbon stocks, NPP, GPP and CUE and turnover rates in Tambopata. A key consideration was assignment and propagation of uncertainty in our measurements. There were two primary types of uncertainty. Firstly, there was sampling uncertainty associated with the spatial heterogeneity of the study plot and the limited number of samples. Examples include the variability among litter traps, or among fine root ingrowth cores. Secondly, there was a systematic uncertainty associated with either unknown biases in measurement, or uncertainties in scaling measurements to the plot level. Examples of unknown biases included the possibility of soil-derived $CO_2$ in the transpiration stream affecting the stem $CO_2$ efflux measurements, and uncertainties in scaling include the allometry of scaling of bole stem $CO_2$ efflux to whole-tree stem respiration, or leaf dark respiration to whole-canopy dark respiration. Here we assumed that most NPP terms were measured fairly precisely and sampled without large biases; hence the NPP component measurements were dominated by sampling uncertainty, which could be reliably estimated, assuming a normal distribution. On the other hand, some of the main autotrophic respiration terms were dominated by systematic uncertainty. This systematic uncertainty can be very hard to reliably quantify; here, in each case we made an explicit and conservative estimate of the systematic uncertainty of key variables.

All estimated fluxes reported in this study are in Mg C ha$^{-1}$ year$^{-1}$ (or month$^{-1}$ for seasonal fluxes) and all reported errors are $\pm 1$ s.e.; error propagation was carried out for all combination quantities using standard rules of quadrature (Hughes and Hase 2010), assuming that uncertainties were independent and normally distributed. One Mg C ha$^{-1}$ year$^{-1}$ is equal to 100 g C m$^{-2}$ year$^{-1}$, or 0.264 µmol C m$^{-2}$ s$^{-1}$. Seasonal shifts in carbon components (e.g. litterfall, root production, NPP, GPP, CUE and turnover rates) between the two plots were analysed by using repeated-measures analysis of variance (ANOVA). Student's *t*-tests were used to assess mean annual differences between the two plots.

### Results

For conciseness, in the following text when values are given for the two plots separated by an oblique sign (/), the first value refers to TAM-05 and the second to TAM-06.

### Climate

The site had moderate seasonality in rainfall (Figure 1), ranging from over 200 mm month$^{-1}$ at the peak of the rainy season (December–February) to less than 100 mm month$^{-1}$ for the 4–5-month dry season of the year (May–September). There was also seasonality in solar radiation, with higher values in the late dry and early wet season (August–November). There was little seasonality in air temperature or relative humidity, though the latter did decline a little in the late dry season. Coolest temperatures were in the austral winter (May–July), when there were occasional incursions by polar fronts (termed *friajes* in Peru, *surazos* in Bolivia, *friagens* in Brazil) that could cause temperatures to dip as low as 5 °C. These lasted only a few days and caused the mean monthly winter temperature to only dip by 1–2 °C (Figure 1). The mean annual rainfall over the period was ca. 1900 mm; this may be lower than the long-term mean because of droughts in 2005 and 2010 (Lewis et al. 2011). The mean annual air temperature was 24.4 °C and mean annual solar insolation was 4.8 GJ year$^{-1}$ m$^{-2}$. Soil moisture content (top 30 cm) was lower in TAM-05 (21.8 $\pm$ 0.18%) than in TAM-06 (35.5 $\pm$ 0.39%), varying from peak values of around 45%/30% in the wet season to minima around 22%/18% in the dry season. The contrast in soil moisture probably reflects differences in soil physical properties: TAM-05 had much higher sand content than TAM-06 (40% vs. 2%; Table 1) and thus lower soil water retention capacity (Table 1). The mean MCWD was calculated to be 259 mm, indicating a substantial dry season (Malhi et al. 2009).

### Above-ground woody biomass and productivity

Mean wood density was 0.61 g cm$^{-3}$ for TAM-05 and 0.51 g cm$^{-3}$ for TAM-06; the lower value at TAM-06
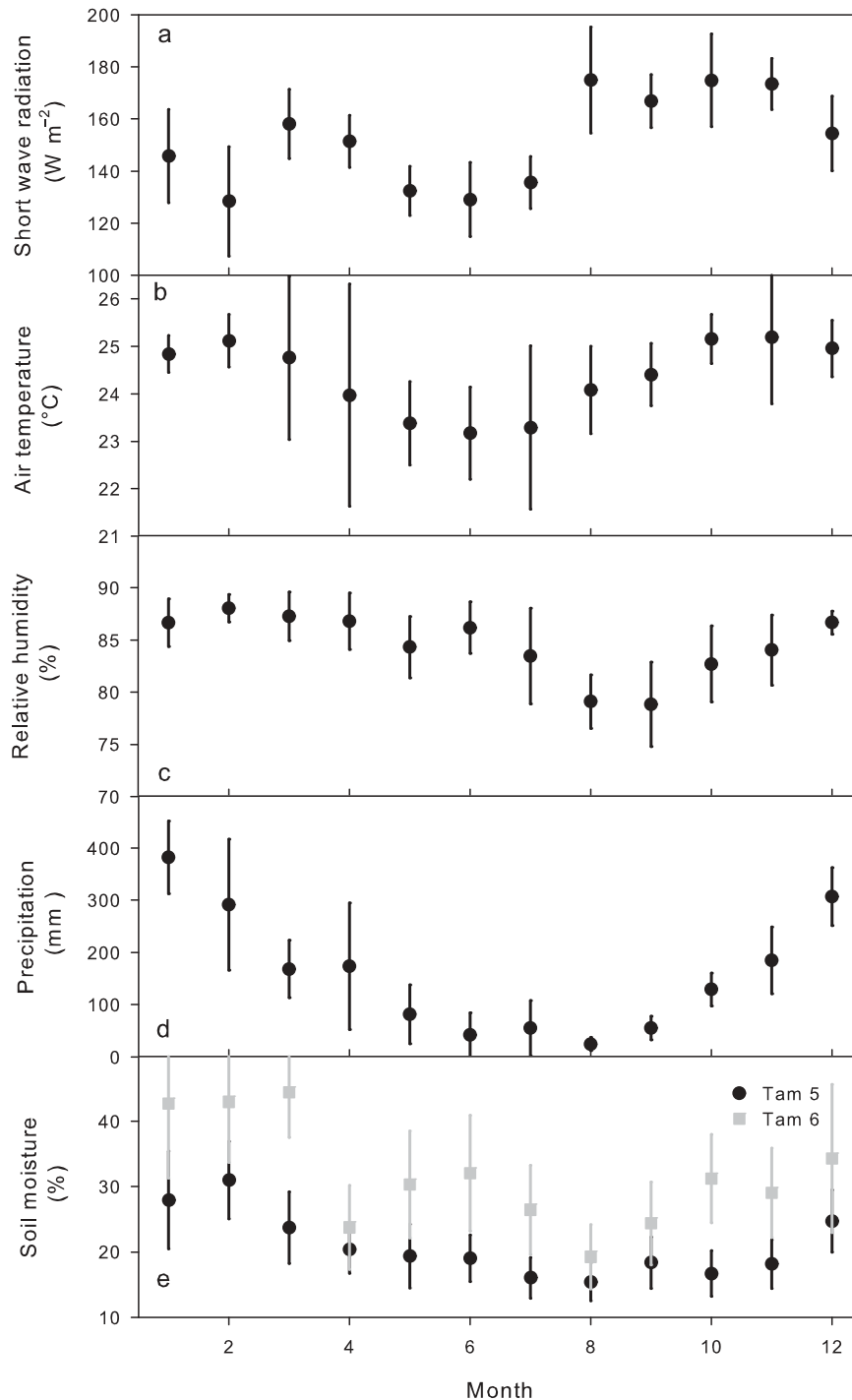
Figure 1. Climate data for the Tambopata field site, showing the mean seasonal cycle over the period March 2005 to December 2011: (a) mean solar radiation; (b) mean monthly air temperature (2 m above ground); (c) mean atmospheric relative humidity (2 m above ground); (d) mean total monthly precipitation (mm); (e) soil moisture volumetric water content (%) in the forest over the depth 0–30 cm.

was strongly influenced by the predominance of *Iriartea* and *Socratea* palms. The basal area-weighted wood density was 0.59/0.50 g cm$^{-3}$. The mean height of canopy trees ($\geq$ 40 cm DBH) was 25.5 $\pm$ 7.8 / 27.6 $\pm$ 8.7, and total above-ground biomass for trees $\geq$ 10 cm DBH was 133.3/109.1 Mg C ha$^{-1}$. There were 210 palms (>10 cm DBH) at TAM-06 with a total woody biomass of 16 Mg C ha$^{-1}$ and 492 dicot trees with a total biomass of

93 Mg C ha$^{-1}$. This low biomass of palms is partially due to their very low wood density, which averages 0.28 g cm$^{-3}$. There were only 23 palms at TAM-05, with a total biomass of 2.5 Mg C ha$^{-1}$. Total stand-level biomass for small trees (< 10 cm DBH) was 4.9/6.5 Mg C ha$^{-1}$. Hence total stand-level above-ground biomass was 138.2/115.6 Mg C ha$^{-1}$, substantially lower at the palm-rich TAM-06 than at TAM-05.

Over the 6 years 2005–2010, we calculated the mean above-ground wood productivity of stems $\geq$ 2.5 cm DBH to be $2.64 \pm 0.24/2.64 \pm 0.25$ Mg C ha$^{-1}$ year$^{-1}$ (Table 4). Of this productivity, 10%/6% accounted for by trees < 10 cm DBH, a component often neglected. To estimate the effect of moisture expansion during the wet season on tree growth estimates, we separated the live trees with almost no annual tree growth (woody NPP < 0.05 kg C tree$^{-1}$, $N = 34$ for TAM-05, $N = 93$ for TAM-06) and calculated the mean seasonal trend in apparent growth. As there was no long-term growth we reasoned that any apparent growth in the rainy season would be a measure of bark or vessel expansion in the rainy season. On these slow-growing trees the mean seasonal amplitude peaked in July and was lowest in October. We estimated a negligible seasonal effect of moisture: 0.005 Mg C ha$^{-1}$ month$^{-1}$ at TAM-05 and 0.002 Mg C ha$^{-1}$ month$^{-1}$ at TAM-06 between April and November. This approach may have underestimated the required correction if fast-growing trees experienced greater dry season contraction than the average (e.g. because of larger vessel size). Even after correcting for moisture expansion, there was a strong seasonality to woody NPP in TAM-06, with a peak in woody growth in December of $0.30 \pm 0.03$ Mg C ha$^{-1}$ month$^{-1}$ and a minimum in woody growth in August of $0.16 \pm 0.02$ Mg C ha$^{-1}$ month$^{-1}$, a halving in growth rates. TAM-05 showed a similar pattern, but with a smaller wet season peak of $0.25 \pm 0.02$ Mg C ha$^{-1}$ month$^{-1}$ and an identical dry season minimum to that in TAM-06 (Figure 2). The average rate of recruitment into the 10 cm DBH size class was 0.07/0.13 Mg C ha$^{-1}$ year$^{-1}$. Because we estimated the productivity of small trees (2.5–10.0 cm DBH) directly, we did not include recruitment in our estimate of total wood productivity. Dividing the above-ground biomass by the stem productivity, we estimated a stem biomass residence time of 52 years for TAM-05 and 43 years for TAM-06,

consistent with the previously noted pattern of smaller residence times in western Amazonia vs. eastern Amazonia, where residence times tend to be 70–100 years (Galbraith et al. 2013). If residence time is calculated only for stems > 10 cm DBH (the most common estimate in forest plots: Malhi et al 2006, Galbraith et al. 2013), the calculated values are 55 and 43 years, respectively. Hence inclusion of small trees has only a modest effect on calculated residence time.

### Litterfall net primary productivity, NPP$_{litterfall}$ and branch turnover, NPP$_{branch\ turnover}$

Litterfall rates were high at both plots: $5.39 \pm 0.35$ and $4.94 \pm 0.40$ Mg C ha$^{-1}$ year$^{-1}$ (Figure 3; Table 4). In terms of litter fractions for TAM-05/06, the litterfall was 74%/72% leaf fall, 3%/4% flower fall, 5%/9% fruit fall, and 17%/15% twig fall. The most significant difference in litter fractions was the much greater fruit production at TAM-06. Based on the 3-monthly transects, the total annual branch turnover NPP averaged $0.95 \pm 0.10 / 0.50 \pm 0.05$ Mg C ha$^{-1}$ year$^{-1}$ (Table 2).

Leaf fall showed substantial seasonality in both plots (Figure 3), beginning to rise in the mid-dry season (July) and peaking at the end of the dry season/start of the wet season (September/October). As the litterfall time series covered more than 5 years there is high confidence in the observed seasonal cycle. Flower fall (Figure 3(c)) peaked in the early wet season (November), with a secondary peak (especially in TAM-06) in the late wet season (April/May). Fruit fall (Fig 3(b)) peaked 2–3 months after the flower fall peak, in February, but only in TAM-06. This brief wet season peak in TAM-06 accounted for most of the larger annual fruit production at this plot. Twig fall (Figure 3(d)) showed no pronounced seasonal pattern; neither did branch fall (Figure 3(e)).
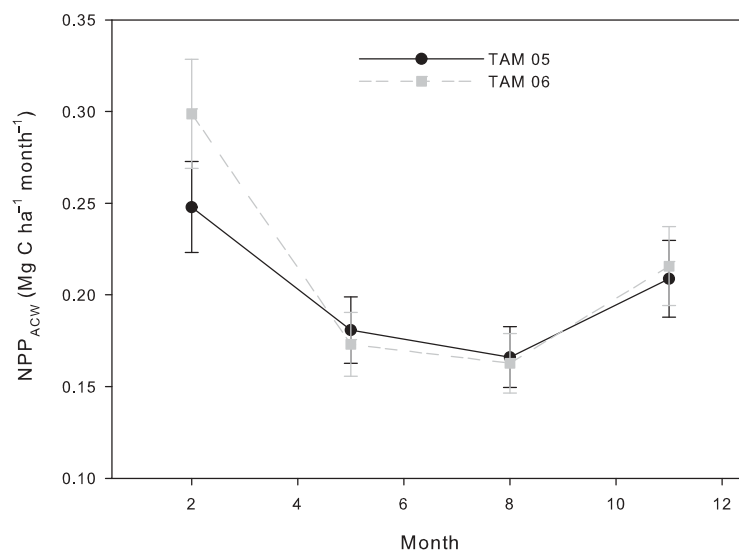


Figure 2.  Mean seasonal cycle of above-ground woody net primary productivity, $NPP_{ACW}$, (Mg C ha$^{-1}$) for the Tambopata plots TAM-05 (black) and TAM-06 (grey).
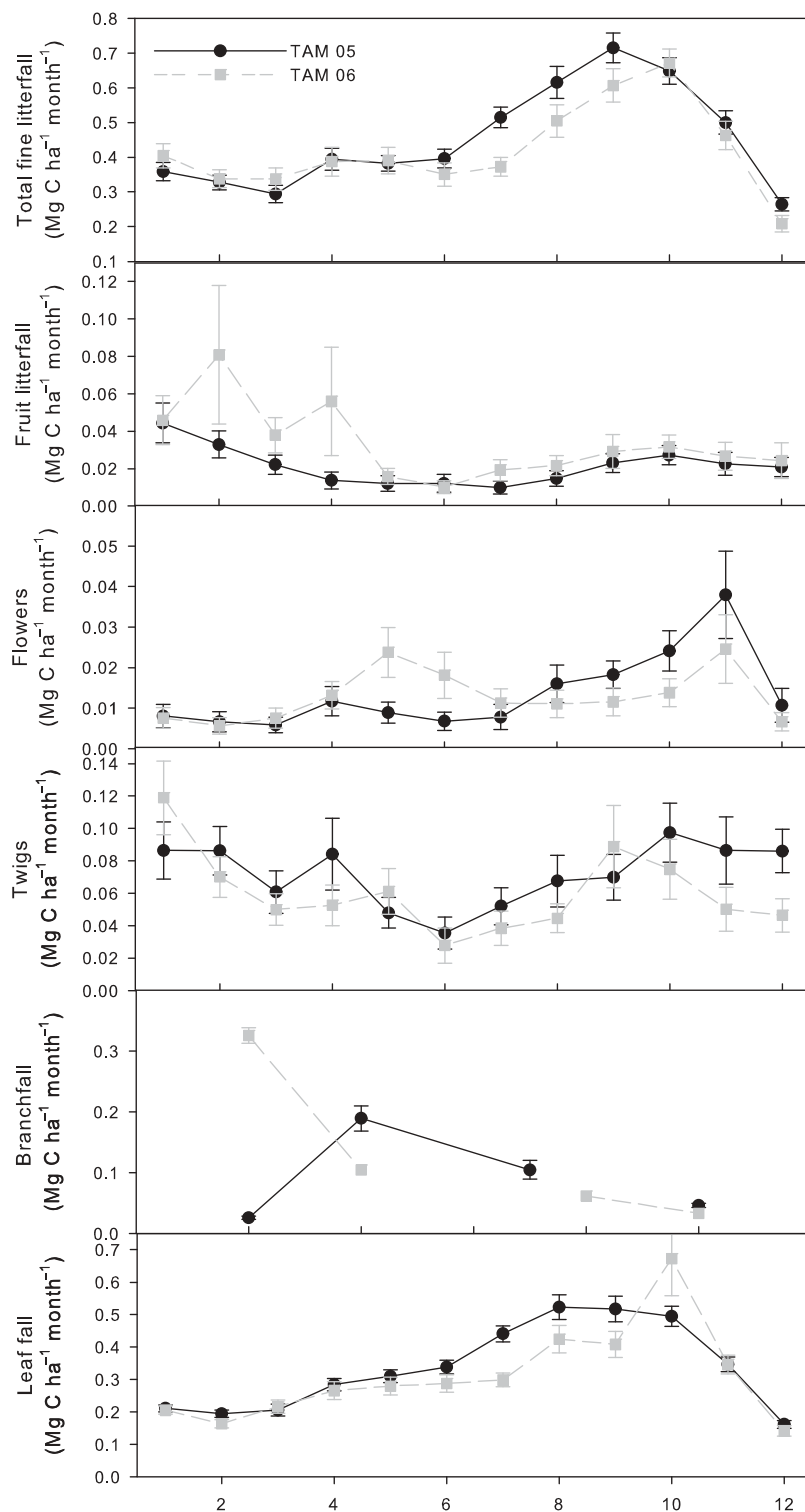
Figure 3. The mean seasonal cycle in canopy litterfall and its components for TAM-05 (grey) and TAM-06 (black): (a) total canopy fine litterfall (as measured in litter traps); (b) fruit fall; (c) flower fall; (d) twig fall (< 2 cm DBH); (e) branch fall (≥ 2 cm DBH; measured along transects and not in litter traps); (f) leaf fall.

### Fine root NPP

Based on the observed exponential decrease in separated fine root material per 10 min sampling period (Metcalfe et al. 2010), we estimated that an additional 24% of fine root material remained uncollected in each ingrowth core in the TAM-05 plot and 23% in the TAM-06 plot, following our standardised 40 min root sampling period. We also estimated that there was an additional 39% fine root NPP beneath our 30 cm ingrowth core, by extrapolating to 1 m depth, assuming an exponential decay of root biomass and
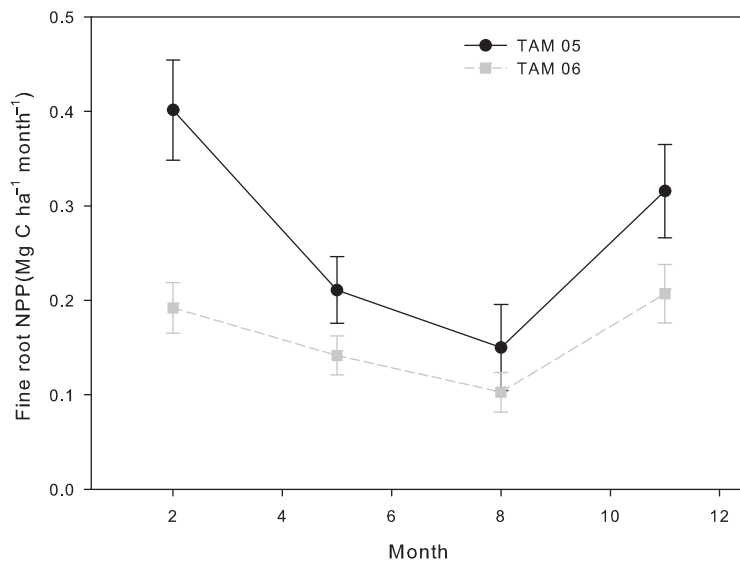
Figure 4.   Mean seasonal cycle of fine root NPP (Mg C ha$^{-1}$ yr$^{-1}$) from 16 ingrowth cores collected every three months for TAM-05 (black) and TAM-06 (grey). Error bars show $\pm 1$ SE.

productivity with depth. Total fine root growth for the TAM-05 plot averaged $4.54 \pm 0.71$ Mg C ha$^{-1}$ year$^{-1}$ but was less than half this value ($2.11 \pm 0.31$ Mg C ha$^{-1}$ year$^{-1}$) at TAM-06 (Table 4). Fine root growth showed substantial seasonality in TAM-05 (Figure 4) in phase with the rainfall pattern, with a peak of $0.40 \pm 0.05$ Mg C ha$^{-1}$ month$^{-1}$ in the peak wet season (January–March), and a minimum of $0.15 \pm 0.05$ Mg C ha$^{-1}$ month$^{-1}$ in the dry season (July–September), more than halving in production rates. TAM-06 showed a similar seasonal pattern in fine root growth but much smaller amplitude.

### Loss to leaf herbivory, $NPP_{herbivory}$

We recorded a mean herbivory fraction of $18.8 \pm 1.3\%$ ($n = 25$) in TAM-06. Correcting the measured $NPP_{leaf}$ in both plots according to this fraction, we estimated an NPP loss to leaf herbivory of $0.76 \pm 0.05$ / $0.70 \pm 0.06$ Mg C ha$^{-1}$ year$^{-1}$ for TAM-05/TAM-06. This relatively large term emerges from a combination of the high herbivory fraction and the high leaf production rates.

### Leaf area index and seasonality of leaf production

The mean leaf area index (LAI) in TAM-05 (Figure 5(a)) peaked at around 5.6 in the wet season and early dry season (February–May), then declined to a value of about 5.0 in the late dry season and early wet season (July–December), and in TAM-06 varied between 5.5 in the wet season and early dry season (January–June), then also declined to a value of about 5.0 in the late dry season and early wet season (July–December). The specific leaf area of canopy leaves was $116 \pm 3/108 \pm 3$ cm$^2$ g$^{-1}$ ($n = 27/28$; S. Patiño, unpublished data). The changes in

LAI and leaf litterfall enabled the estimation of the seasonal cycle of leaf production (Figure 5(b), (c)). At both sites, leaf shedding (litterfall) began in May/June, matched by a decline in LAI. By August, LAI halted its decline despite a further steep rise in leaf fall rates, indicating that the production of new leaves was balancing the loss of old leaves (Figure 5(b), (c)). Overall, leaf production showed a distinct peak at both sites in the late dry season (August–October), which also matched the peak in leaf fall rates, indicating high rates of leaf shedding and replacement in this period. Minimum leaf production appeared to be in the early dry season (May–July), particularly in TAM-06.

### Palm leaf and fruit productivity

Overall, we estimated $NPP_{palm}$ (leaves and reproductive structures only) to be $0.22 \pm 0.07$ Mg C ha$^{-1}$ year$^{-1}$ for TAM-05, and $2.81 \pm 0.84$ Mg C ha$^{-1}$ year$^{-1}$ for TAM-06 (we assigned 30% errors to these estimates because of the considerable systematic uncertainty). The seasonal cycle of palm fruit fall showed a distinct peak in December–March, suggesting a peak in palm fruit production over November–March (early-mid wet season), and a near-zero minimum in May–July (early-mid dry season). As this pattern was similar to that of the dicot-dominated $NPP_{canopy}$ (see below), we assumed that at seasonal level the NPP of palm reproductive structures was a fixed multiplier of the measured (dicot) NPP for flowers and fruit. We had no data on the seasonality of palm leaf productivity but likewise assumed a fixed multiplier of dicot $NPP_{leaf}$. The multiplier was calculated from the annual total and for TAM-05/TAM-06 palm leaves was 1.02/1.31, and for palm fruit was 1.19/2.35.
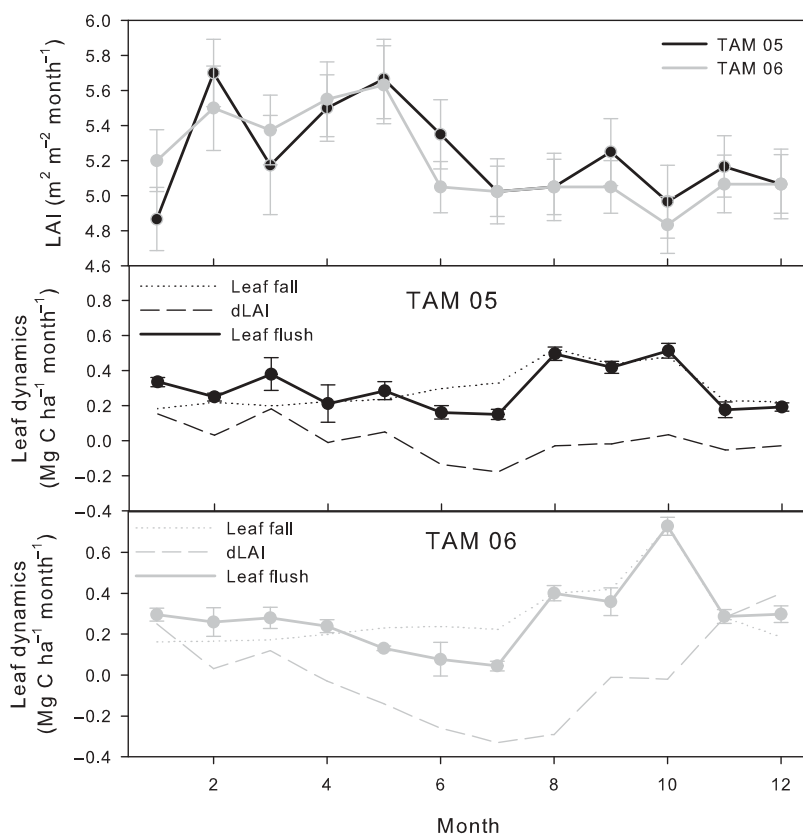
Figure 5. Mean seasonal cycle of (a) Leaf area index (LAI) (m² m⁻²) calculated from 25 hemispherical photos taken every month; (b) the leaf production and shedding budget for TAM-05; c) the leaf production and shedding budget for TAM-06. Error bars indicate standard errors of the mean.

*Respiration*

*Soil respiration and its partitioning.* We found no evidence of a net disturbance effect on our partitioning experiment at this site (see supplemental material). Averaged monthly values of estimated rhizosphere respiration at TAM-05 were 40% of total soil respiration. This fraction varied seasonally with dry season values (June–October) averaging 34% and the rest of the year averaging 44%. Averaged monthly values at TAM-06 were 42% of soil respiration. This fraction also varied seasonally, with June–October values averaging 39% and the rest of the year averaging 45% (Figure 6).

Total soil respiration had a significant seasonal cycle ($P < 0.001$) and was lowest in the dry season (between May and September) at both sites. Total soil respiration over the 25 sample points per plot was not significantly different between sites ($P > 0.05$) and averaged $12.11 \pm 0.60/10.97 \pm 0.54$ Mg C ha⁻¹ year⁻¹ at TAM-05/TAM-06. Total rhizosphere respiration had a significant seasonal cycle ($P < 0.001$) and was also lowest in the dry season. Annual mean rhizosphere respiration was not significantly different between sites ($P > 0.05$) and averaged $5.07 \pm 0.61/4.62 \pm 0.57$ Mg C ha⁻¹ year⁻¹. Total heterotrophic soil respiration had a significant seasonal cycle ($P < 0.001$) and was highest in the late dry season. This coincided with the time of maximum litterfall (Figure 3) and fresh organic matter inputs. Annual mean soil heterotrophic respiration

$7.08 \pm 0.86/6.34 \pm 0.76$ Mg C ha⁻¹ year⁻¹ in the two plots.

*Above- and below-ground live stem $CO_2$ flux, $R_{stem}$ and $R_{coarse\ root}$.* The total woody surface area of trees $\geq 10$ cm DBH at was calculated to be 18,400/19,700 m² ha⁻¹ and for small trees (2.5–10.0 cm diameter) was 1400/1200 m² ha⁻¹. This summed to a stem area index of 1.98/2.09 for the two sites. Woody respiration per unit stem area was not significantly different between the plots, averaging $0.95 \pm 0.03$ μmol m⁻² s⁻¹ at TAM-05 compared with $1.03 \pm 0.08$ μmol m⁻² s⁻¹ for TAM-06.

To scale these measurements to the plot level we looked for a relationship between above-ground woody growth ($NPP_{ACW}$) per tree and stem $CO_2$ flux for these 25 trees. There was a significant positive linear relationship between $NPP_{ACW}$ and stem $CO_2$ flux for both plots. The best-fit equation for TAM-05 was: stem $CO_2$ flux $= 120 \times NPP_{ACW} + 0.84$; and for TAM-06: stem $CO_2$ flux $= 45 \times NPP_{ACW} + 0.97$ with $NPP_{ACW}$ in Mg C ha⁻¹ month⁻¹ and stem $CO_2$ flux in μmol m⁻² s⁻¹. We scaled these equations to the whole plot and found that the trees sampled for stem $CO_2$ flux grew faster than average, and therefore we had to reduce our estimates for respiratory fluxes by 5% at TAM-05 and 4% at TAM-06 when scaled to the entire plot. We also used continuous soil surface temperatures (a proxy for woody surface temperature) to scale temporally from
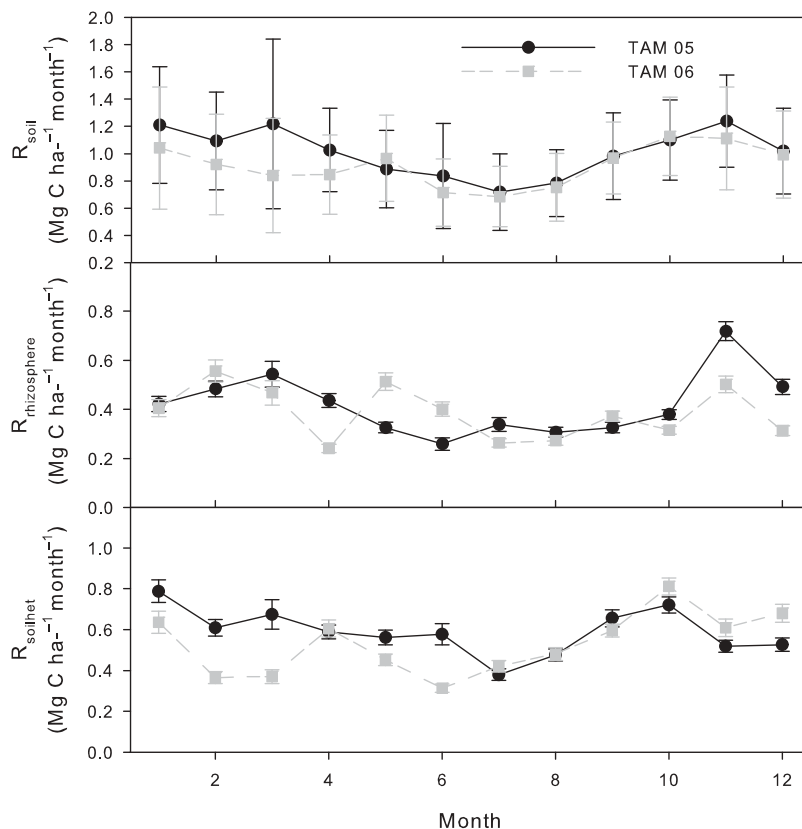
Figure 6.    Mean seasonal cycle of (a) total soil $CO_2$ efflux from 25 collars measured monthly; (b) rhizosphere respiration; (c) heterotrophic soil respiration Error bars indicate standard errors of the mean.
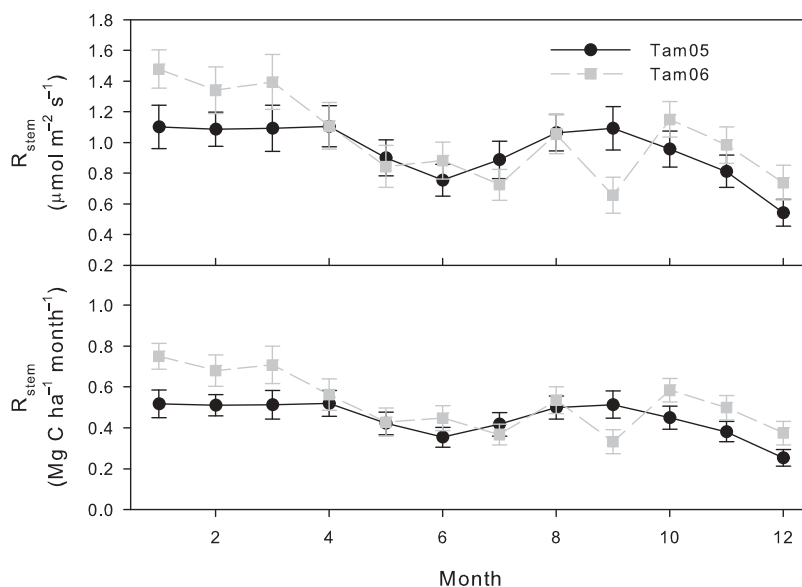


Figure 7.    Means seasonal cycle of (a) The respiration rate per unit stem area as measured for 25 trees in each plot; (b) the same respiration measures scaled by wood surface area to above-ground live wood respiration rates per hectare. Error bars show $\pm 1$ SE.

the time of measurements to the whole diurnal, seasonal and annual cycle.

We then multiplied total plot woody surface area by our scaled stem $CO_2$ fluxes (Figure 7). There was a significant seasonal cycle ($P < 0.001$) in stem $CO_2$ flux at both sites. In TAM-05, stem $CO_2$ flux showed a broad

peak in the wet season (January–March), but a second similar broad peak in the late dry season (August–October). In TAM-06 there was a more distinct peak in the wet season (January–March). Total annual above-ground woody respiration for the two plots was estimated to be $5.43 \pm 1.77 / 7.62 \pm 2.48$ Mg C ha$^{-1}$ year$^{-1}$ (Table 4).

Using a simple multiplier of above-ground wood respiration, we estimated coarse root respiration (i.e. below-ground woody respiration) to be $1.14 \pm 0.59/1.60 \pm 0.82$ Mg C ha$^{-1}$ year$^{-1}$ (Table 4).

*Canopy leaf respiration (R$_{leaf}$).* Leaf dark respiration values were significantly higher at TAM-05 relative to TAM-06 for both seasons, and for sun and shade leaves (Table 5). There was only slight seasonality; shade leaf respiration values were significantly higher in the wet season (measured at TAM-06 only), and in both plots sun leaf respiration values were not significantly different between seasons. In the dry season, sun leaves had higher leaf respiration rates than shade leaves (measured at TAM-06 only), but in the wet season there was no significant difference between sun and shade leaves. When scaled up to the whole canopy, there was little seasonality in our estimated canopy leaf respiration. We did not find a significant relationship ($P > 0.05$) between trunk NPP and leaf dark respiration of individual trees. After multiplying by $0.67 \pm 0.15$ to account for light inhibition of dark respiration, total annual canopy respiration was estimated to be $8.86 \pm 2.84$ Mg C ha$^{-1}$ year$^{-1}$ at TAM-05 and $6.43 \pm 2.07$ Mg C ha$^{-1}$ year$^{-1}$ at TAM-06 (Table 4).

### NPP, GPP and CUE

The measured and estimated components of NPP were summed using Equations 1 and 2 to estimate a plot-level NPP of $15.0 \pm 0.8$ Mg C ha$^{-1}$ year$^{-1}$ for TAM-05 and $14.2 \pm 1.0$ Mg C ha$^{-1}$ year$^{-1}$ for TAM-06. The four estimated components of autotrophic respiration were summed using Equation 3 to estimate total autotrophic respiration at $20.5 \pm 3.5/20.3 \pm 1.3$ Mg C ha$^{-1}$ year$^{-1}$. The sum of NPP and autotrophic respiration gave an estimated GPP of $35.5 \pm 3.6/34.5 \pm 3.5$ Mg C ha$^{-1}$ year$^{-1}$. The ratio of NPP to GPP gave an ecosystem CUE of $0.42 \pm 0.05/0.41 \pm 0.05$ (Table 4).

### Allocation

The total allocation (of NPP and autotrophic respiration combined) was similar in both plots, with $32 \pm 3 / 28 \pm 4\%$ being allocated below ground (Table 6). Considering only NPP there were significant differences between the sites. There was greater NPP allocation to fine roots in TAM-05 ($30 \pm 5\%$ vs. $15 \pm 2\%$) offset by greater allocation to canopy in TAM-06. Allocation to woody production was similar in both plots ($27 \pm 6 / 26 \pm 5\%$).

## Discussion

### Variation of NPP and its components over the seasonal cycle

In this paper we have quantified the main components of NPP for two plots in the Tambopata lowland Amazonian forest, and described their variation over the seasonal cycle. By combining leaf litterfall and LAI data, we have also quantified the seasonal cycle of leaf production. This enables us to explore the seasonal variation of NPP and its allocation, the first time this has been done for a tropical forest.

Fine root NPP, above-ground woody NPP and leaf NPP make up most of the NPP budget, but for completeness we also made assumptions about the seasonal variation of the remaining components. We assumed that $NPP_{\text{branch turnover}}$, $NPP_{\text{ACW <10 cm}}$, and $NPP_{\text{coarse roots}}$ followed the same seasonal cycle as $NPP_{\text{ACW} \geq 10\,\text{cm}}$, and used a multiplying factor of $1.80 \pm 0.08/1.52 \pm 0.05$ for TAM-05/06, based on the annual ratio of these terms (Table 4). For the canopy NPP terms we (i) assumed that the majority of flower and fruit NPP were equal to measured flower and fruit fall, as these components probably have canopy lifetimes less than 3 months; (ii) twig NPP had no seasonal variation as twig fall shows no seasonality; (iii) leaf NPP lost to herbivory tracked leaf NPP as a multiplying factor of 1.18 for both plots, based on the measured herbivory fraction. For palm fruit, as the seasonal pattern is similar to that of $NPP_{\text{canopy}}$, we assumed that at seasonal level the NPP of palm leaves and reproductive structures tracked the dicot $NPP_{\text{canopy}}$.

In TAM-05 (Figure 8(a)), NPP showed substantial seasonal variation, ranging from $1.48 \pm 0.07$ Mg C ha$^{-1}$ month$^{-1}$ in the mid-wet season (January–March), and declining to $0.83 \pm 0.07$ Mg C ha$^{-1}$ month$^{-1}$ in the wet–dry transition (April–June). In TAM-06 (Figure 8(b)) the seasonality was even more pronounced, ranging from $1.90 \pm 0.30$ Mg C ha$^{-1}$ month$^{-1}$ in the dry–wet transition season to $0.69 \pm 0.31$ Mg C ha$^{-1}$ month$^{-1}$ in the wet–dry transition. In both plots NPP was lowest in the wet–dry transition, rather than in the mid-late dry season (July–September), when water stress would be expected to have its greatest impact on GPP.

In terms of relative allocation (Figure 8(c); Table 5), there were interesting differences between the plots. In TAM-05 (the much sandier site; Table 1) the components with the greatest seasonal variation in allocation were leaf and fine root NPP, with allocation to leaf production peaking in the late dry season when allocation to fine roots was at a minimum. This suggests that a trade-off between carbon allocation to fine roots vs. leaves is associated with the late dry season leaf flush. The peak in production of leaves in the late dry season was consistent with satellite observations of canopy greening in Amazon forests in the dry season (e.g. Anderson et al. 2010).

In TAM-06 the relative allocation pattern was somewhat different (Fig 8(d)). Fine root and wood production showed moderate seasonality, with a minimum in the dry season (Figure 8(b)). There appeared to be a large investment in canopy production in the dry–wet transition (October–December), although not at the expense of a decline in other NPP components.

### Variation of respiration and total plant carbon expenditure over the seasonal cycle

In addition to the components of NPP, we were able to describe the seasonal variation in the main components of
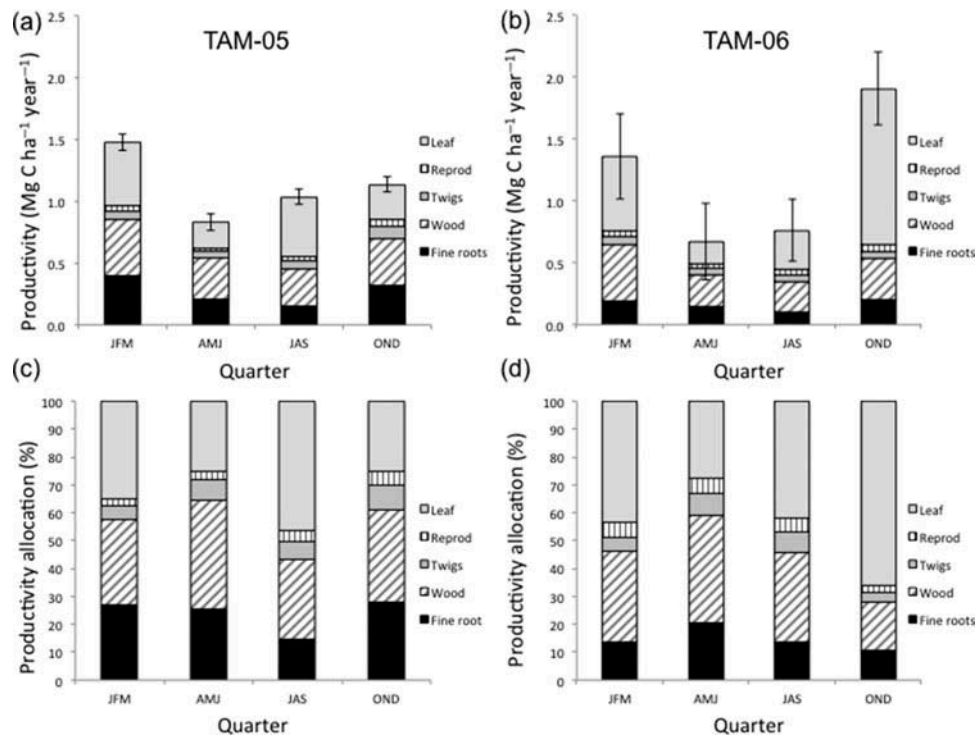
Figure 8.    The seasonal cycle of NPP and its components: (a) for TAM-05, showing the absolute values; (b) for TAM-06, showing the absolute values; (c) for TAM-05, showing the proportional allocation; (d) for TAM-06, showing the proportional allocation.

autotrophic respiration. The sum of the autotrophic respiration and NPP is equivalent to the total PCE (Metcalfe et al. 2010). On a seasonal timescale we distinguish PCE from GPP, as there is likely to be significant seasonal storage of carbon in the form of non-structural carbohydrates (Wurth et al. 2005). On an annual basis in a near-equilibrium system, PCE should be approximately equal to GPP.

Total autotrophic respiration showed no significant seasonality ($P > 0.10$) in both sites (Figure 9). In TAM-05 it ranged from $2.32 \pm 0.82$ Mg C ha$^{-1}$ year$^{-1}$ in the wet season to $2.02 \pm 0.69$ Mg C ha$^{-1}$ year$^{-1}$ in the dry season (Figure 9(a)). In TAM-06 the seasonality appears stronger but still not significant, ranging from $2.44 \pm 0.92$ Mg C ha$^{-1}$ year$^{-1}$ in the wet season to $2.64 \pm 0.59$ Mg C ha$^{-1}$ year$^{-1}$ in the dry season (Figure 9(b)). There was remarkably little seasonal variation in the partitioning of autotrophic respiration throughout the year. In TAM-05 there is a suggestion of a slight decline in allocation to rhizosphere respiration in the dry season. The apparent lack of seasonality of leaf respiration should be treated with caution; our limited seasonal sampling of this term means that there might have been periods (e.g. the late dry season leaf flush, with plentiful young leaves with higher respiration rates) that have been missed by our sampling.

The total PCE showed moderate seasonality, driven mainly by the large seasonality in NPP rather than the slight seasonality in autotrophic respiration. In TAM-05 it ranges from $3.80 \pm 0.82$ Mg C ha$^{-1}$ month$^{-1}$ in the wet season to $2.87 \pm 0.73$ Mg C ha$^{-1}$ month$^{-1}$ in the dry season. In TAM-06 it ranges from $3.83 \pm 0.98$ Mg C ha$^{-1}$ month$^{-1}$

in the wet season to $2.40 \pm 0.64$ Mg C ha$^{-1}$ month$^{-1}$ in the dry season. It remains to be determined whether this is an indicator of seasonality in GPP, or whether there is substantial seasonal variation in non-structural carbon (NSC) reserves (Wurth et al. 2005), with excess PCE in the wet season being supported by non-structural reserves, which are then replenished in the dry season. The low variation in light availability (Figure 1) and in leaf area across the seasons (Figure 5(a)) suggests that seasonal variation in NSC reserves, rather than variation in canopy photosynthesis, is the predominant determinant of seasonality in PCE and NPP. The amplitude of the seasonality in PCE (Figure 9) suggests that the minimum size of the seasonally labile storage pool is about 3 Mg C ha$^{-1}$. The suggested pattern of NSC accumulation in the dry season and depletion in the wet season is consistent with a direct measurement of seasonal variation in the NSC pool in Panama (Wurth et al. 2005), and the estimated seasonal amplitude of pool size here is very similar that observed in Panama ($3.2$ Mg C ha$^{-1}$ seasonal variation in a total NSC pool of $16.1$ Mg C ha$^{-1}$, derived from the information in Wurth et al. 2005). The Panama analysis suggests that 70% of this seasonal variation is in NSC reserves in branches and stem wood. The importance and seasonal variation of the NSC pool suggests that much of seasonal variation in NPP and woody growth may be decoupled from seasonal variation in GPP.

The CUE (here defined as NPP/PCE at seasonal timescales) suggests similar seasonality in both plots, though the high uncertainty assigned to autotrophic respiration estimates limits significance. In the context
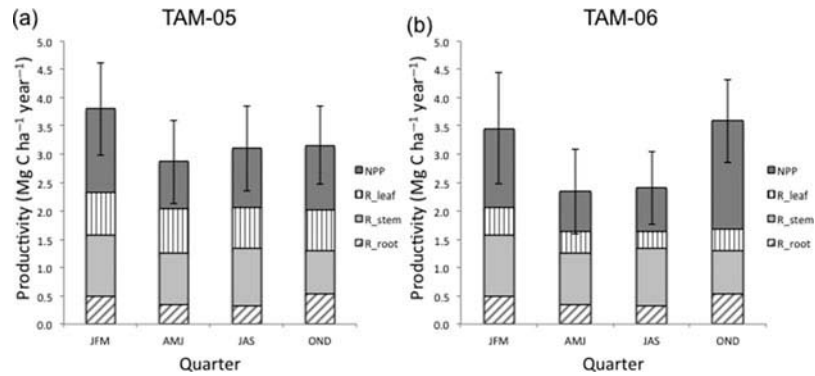
Figure 9. The seasonal cycle of total NPP, the components of autotrophic respiration, and total plant carbon expenditure for (a) TAM-05 and (b) TAM-06.

of comparisons between seasons, we have probably overestimated uncertainty in $R_a$ as the scaling factors are not likely to vary much between seasons. CUE is highest in the wet season (October–March), being $0.37 \pm 0.06/0.44 \pm 0.09$ in TAM-05/06, and reaches its lowest values in the wet–dry transition (April–June), being $0.29 \pm 0.08/0.27 \pm 0.08$. Overall, this suggests the trees invest relatively more in NPP in the October–March period, and relatively more in maintenance in the April–September period. The fact that the minimum is in the wet–dry transition suggest that this pattern is driven by phenological rhythms rather than being directly driven by water stress, which peaks later in the dry season.

*The carbon budget of the Tambopata plots*

For the first time we are able to present a carbon budget for a lowland western Amazonian forest site (Table 4, Figure 10). The GPP of the two plots was estimated to be

$35.5 \pm 3.6$ for TAM-05 and $34.5 \pm 3.5$ for TAM-06, with no significant difference between the two plots. This compares with values of 29.9–31.4 Mg C ha$^{-1}$ year$^{-1}$ previously reported for three sites in eastern Amazonia (Malhi et al. 2009), but are only slightly and not significantly higher than more comprehensive recent estimates for sites at Caxiuana, Brazil ($33.0 \pm 5.36$ for a sandy soil, $32.08 \pm 3.46$ for a clay soil (Metcalfe et al. 2010; Doughty et al. 2014). Mercado et al. (2011) tried to estimate the GPP of these two sites using canopy leaf N and P data, and a model of co-limitation of photosynthesis (Domingues et al. 2010). They estimated a GPP of 33.4 Mg C ha$^{-1}$ year$^{-1}$ for TAM-05 and 40.8 Mg C ha$^{-1}$ year$^{-1}$ for TAM-06. These values bracket the field data, but suggest from leaf nutrient considerations that we would have expected TAM-06 to be the more productive plot.

The estimated NPP of the two sites was $15.0 \pm 0.8$ and $14.2 \pm 1.0$ Mg C ha$^{-1}$ year$^{-1}$. This is similar to values previously reported for these sites, using shorter time series by
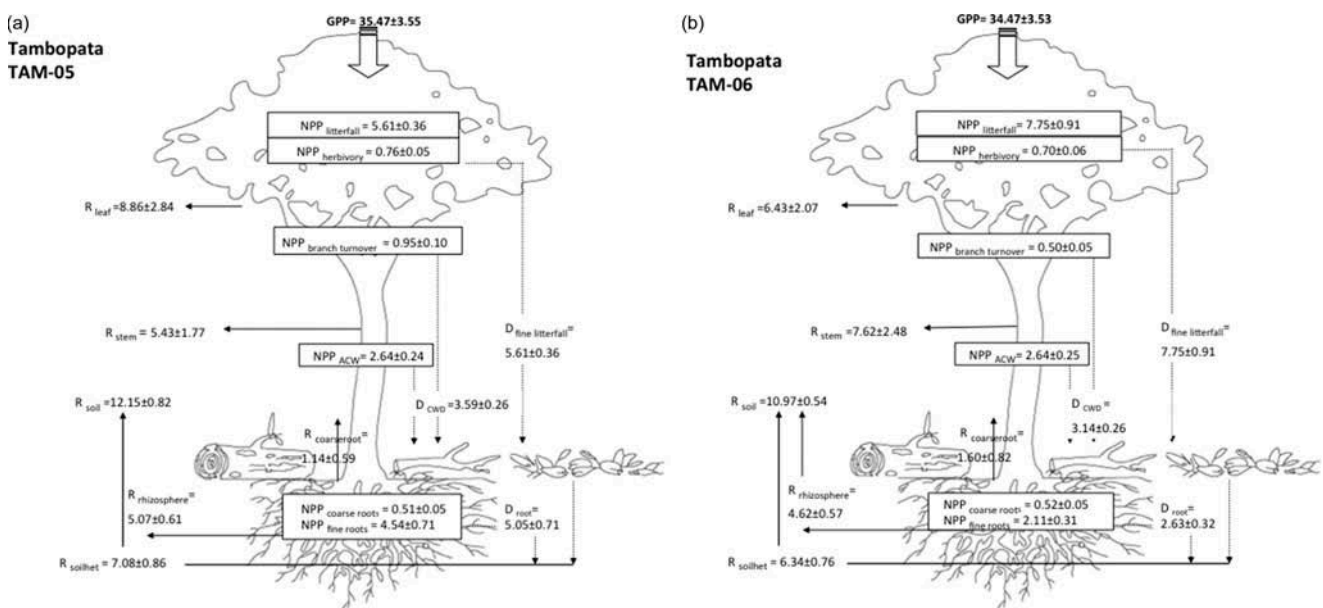


Figure 10. A comprehensive assessment of the mean annual budget of the components of autotrophic respiration, NPP, and GPP for (a) TAM-05 and (b) TAM-06. Here NPP$_{litterfall}$ includes NPP$_{palm}$.

Aragão et al. (2009) (16.9 ± 1.5, 13.9 ± 1.3) and Girardin et al. (2010) (16.9 ± 1.5, 13.6 ± 1.3). In part the differences reflect improved calculation procedures (e.g. local tree height data which reduce estimates of $NPP_{stem}$, and inclusion of palm canopy production) and a longer time series data set. The estimated CUE (0.42 ± 0.05 and 0.41 ± 0.05) was higher than that reported by Malhi et al. (2009) for the undisturbed sites in Brazilian Amazonia (0.32–0.34 for Manaus and Caxiuana), but lower than the value of 0.49 estimated at the relatively disturbed site at Tapajós, Brazil. Malhi et al. (2009) suggested that the value of CUE for Amazonian forests was linked to forest dynamics, that more dynamic forests with more gaps and light penetration favoured faster-growing, high-CUE trees and species with lower biomass and maintenance costs. The forests at Tambopata have faster turnover than their Brazilian counterparts (residence time around 50 years compared with 70–100 years in eastern Amazonia; Phillips et al. 2004; Malhi et al. 2006), probably because of soil fertility or soil structural factors (Quesada et al. 2011, 2012). Hence this higher rate of intrinsic disturbance may have resulted in the higher values of CUE.

In terms of allocation of NPP (Table 5), at both plots the allocation to canopy NPP was highest (42% and 59%) compared with wood (27% and 26%) and fine roots (31% and 15%). The most noteworthy difference between plots was the very high canopy allocation in TAM-06, offset by very low fine root allocation. This almost certainly arose because of the abundance of palms in TAM-06, which have high leaf and fruit investment and low fine root productivity. In the dry season the fine root allocation was similar in both plots (Figure 8(a) and (b)); but in the wet season fine root production increased in TAM-05 but actually decreased in TAM-06. This may be because of the occasional waterlogging of part of the plot in the wet season, creating anoxic conditions unfavourable to root growth. It may also reflect the abundance of palms in TAM-06, which may have very different fine root allocation patterns than dicot trees. Malhi et al. (2011) reviewed reported allocation patterns in 35 tropical forests (including TAM-05 and TAM-06 as reported in Aragão et al. 2009), and found mean allocations

of 34%, 39% and 27% to canopy, wood and fine roots, respectively. The values reported here for the Tambopata plots represent higher allocation to canopy NPP (42% and 59%) than reported for other tropical forests, and thus are outside the distribution of allocation points reported by Malhi et al. (2011). The new values of allocation are substantially different because of the inclusion of a leaf herbivory term (which increases canopy allocation by 3%), palm leaf and fruit production, and a smaller branchfall term (14% of $NPP_{ACW>=10\,cm}$) than previously estimated. Our study includes elements that are rarely reported in NPP studies, including estimates of leaf herbivory, branch fall, and small tree productivity.

The allocation of autotrophic respiration (Table 6) carries greater uncertainty because of the challenges in scaling leaf and especially stem respiration (Levy and Jarvis 1998; Meir and Grace 2002; Cavaleri et al. 2006). Nevertheless, the relative differences between plots may be more robust than the absolute values as identical methods were applied to both sites. The proportion of respiration allocated to wood was much greater than the proportion of NPP, and correspondingly the allocation of respiration to canopy and fine roots was lower than the allocation of NPP to these tissues (Table 6). The high respiration component in live wood may be indicative of the maintenance costs of this large biomass component, which has a large stock even if it is less metabolically active per unit mass than leaf or fine root tissue. The lower biomass plot, TAM-06, dominated by low wood density palms, had the higher wood respiration allocation, possibly because the amount of active live woody tissue may be greater in TAM-06 because of the greater woody surface area. The respiration component in canopy and rhizosphere was similar in the two plots. Another possibility is that the transport of dissolved $CO_2$ in the transpiration stream artificially increases the apparent wood respiration above that arising from local stem respiration (Levy et al. 1999; Teskey and McGuire 2002). If this were the case, we might expect greater apparent allocation to wood respiration in the wet season when soil moisture is abundant and heterotrophic respiration rates are highest. We saw no evidence of such a trend here. It is also possible

Table 6.    Patterns of carbon allocation in the plots in Tambopata, Peru.

| Allocation of total carbon (NPP and respiration) | TAM-05 Mean (±SE) | TAM-06 Mean (±SE) |
|---|---|---|
| Above-ground carbon (Mg C ha$^{-1}$ year$^{-1}$) | 24.03 (±1.30) | 22.81 (±1.32) |
| Below-ground carbon (Mg C ha$^{-1}$ year$^{-1}$) | 11.22 (±0.80) | 8.86 (±0.49) |
| Above-ground fractional allocation | 0.68 (±0.05) | 0.72 (±0.07) |
| Below-ground fractional allocation | 0.32 (±0.03) | 0.28 (±0.03) |
| **Allocation of NPP** | | |
| Canopy fraction | 0.42 (±0.04) | 0.59 (±0.05) |
| Wood fraction | 0.27 (±0.06) | 0.26 (±0.05) |
| Fine roots fraction | 0.30 (±0.05) | 0.15 (±0.02) |
| **Partitioning of autotrophic respiration** | | |
| Canopy fraction | 0.43 (±0.06) | 0.32 (±0.04) |
| Wood fraction | 0.32 (±0.05) | 0.45 (±0.07) |
| Rhizosphere fraction | 0.25 (±0.02) | 0.23 (±0.02) |

that xylem transport of plant respired $CO_2$ would decrease measured stem $CO_2$ efflux. However, the seasonal variation in transpiration at this site may be slight; results from a more seasonal site may help resolve if $CO_2$ transport in the xylem is an important component.

The patterns of higher NPP and GPP were consistent with the Amazonian east–west gradient in productivity that has been associated with soil fertility (Malhi et al. 2004; Quesada et al. 2012). The high CUE appears linked to high productivity and turnover (Malhi et al. 2009; Vicca et al. 2012) – the high turnover may shift forest composition towards lower biomass, early life-stage trees with lower maintenance respiration costs and thus higher CUE, and also favour trees and traits which favour rapid growth over defence. The patterns of NPP allocation differed significant between the plots, with the more fertile plot (TAM-06) having higher allocation to canopy and lower allocation to fine roots. This pattern is consistent with the expectations of resource allocation theory, with more investment in nutrient acquisition at the nutrient-poor site. However, much of this between-site difference may be associated with shifts in functional groups, with an abundance of palms at TAM-06 with high canopy allocation and low root allocation. Palm abundance is often associated with water-logging, and may be linked to occasional water-logging at TAM-06 and the higher water retention in the silt-clay soil at this plot. This suggests that water budgets and soil hydrological properties may drive the differences in allocation between the plots.

## Conclusions

In this study we have presented the first comprehensive carbon cycle description for a forest in western Amazonia, and also the first comprehensive description of seasonal variations in the carbon budget for any tropical forest. The study shows that there are differences in carbon dynamics compared with sites in eastern Amazonia (most notably in CUE) but also some surprisingly small differences (e.g. in GPP).

We have been able to describe the seasonal variation in the components of NPP, autotrophic respiration and plant carbon use for the first time. We have demonstrated substantial seasonality in NPP, but much less seasonality in autotrophic respiration. The observed seasonality in PCE seems likely to be more closely associated with seasonal variation of the NSC pool rather than with seasonal variation in GPP. Overall, the paper demonstrates the power of a comprehensive 'bottom-up' approach to estimating the forest carbon cycle, that complements and greatly extends any information that is available from, for example, carbon dioxide flux towers.

## Notes on contributors

Yadvinder Malhi is Professor of Ecosystem Science, with research interests focussed on the functioning and ecology of tropical forests.

Filio Farfan-Amezquita and Javier Silva-Espejo are Peruvian researchers who were responsible for the collection of the long-term data at Tambopata.

Chris Doughty, Cecile Girardin and Toby Marthews are ecosystem ecologists whose work focusses on analysing the carbon cycle of tropical forests.

Daniel Metcalfe is an ecosystem scientist who works on carbon dynamics in tropical boreal systems.

Luiz Aragão is an ecologist with a focus on carbon dynamics, fires and remote sensing.

Lidia Huaraca-Quispe, Ivonne Alzamora-Taype, Luzmila Eguiluz-Mora, Clara Rojas-Villagra and Yulina Pelaez-Tapia are Peruvian students who participating in field data collection or in processing and separation of litterfall data.

Kate Halladay is a meteorologist with an interest in tropical climate systems and in the analysis of weather station data.

Carlos Alberto Quesada is a Brazilian soil scientist who specialises in the soils of the Amazon forest.

Amanda Robertson is an ecologist who initiated and implemented the measurements of stem respiration.

Joshua Fisher is an ecosystems scientist with an interest in carbon and nutrient cycling in terrestrial biomes.

Joana Zaragoza-Castells is a plant ecophysiologist who collected much of the data on leaf respiration and photosynthesis.

Norma Salinas is a tropical forest ecologist and responsible for the implementation of long-term carbon cycle research at Tambopata.

Patrick Meir is Professor of Ecosystem Science, with a particular interest in tropical ecophysiology and soil carbon dynamics.

Oliver Phillips is Professor of Tropical Ecology and established the long-term forestry inventory plots at the Tambopata site; his interests focus on tropical forest ecology and climate change.

## References

Anderson LO, Malhi Y, Ladle RJ, Aragão LEOC, Shimabukuro Y, Phillips OL, Baker T, Costa ACL, Espejo JS, Higuchi N, et al. 2009. Influence of landscape heterogeneity on spatial patterns of wood productivity, wood specific density and above ground biomass in Amazonia. Biogeosciences 6:1883–1902.

Anderson LO, Malhi Y, Aragão LEOC, Ladle R, Arai E, Barbier N, Phillips OL. 2010. Remote sensing detection of droughts in Amazonian forest canopies. New Phytologist, 187:733–750.

Aragão LEOC, Malhi Y, Metcalfe DB, Silva-Espejo JE, Jimenez E, Navarrete D, Almeida SS, Costa ACL, Salinas N, Phillips OL, et al. 2009. Above- and below-ground net primary productivity across ten Amazonian forests on contrasting soils. Biogeosciences 6:2759–2778.

Atkin OK, Evans JR, Ball MC, Lambers H, Pons TL. 2000. Leaf respiration of snow gum in the light and dark: interactions between temperature and irradiance. Plant Physiology 122:915–923.

Baker TR, Phillips OL, Malhi Y, Almeida S, Arroyo L, di Fiore A, Erwin T, Killeen TJ, Laurance SG, Laurance WF, et al. 2004. Variation in wood density determines spatial patterns in Amazonian forest biomass. Global Change Biology 10:545–562.

Baker T, Honorio CE, Phillips OL, van der Heijden G, Martin J, Garcia M, Silva Espejo JE. 2007. Low stocks of coarse woody debris in a south-western Amazon forest. Oecologia 152:495–504.

Cairns MA, Brown S, Helmer EH, Baumgardner GA (1997). Root biomass allocation in the world's upland forests. Oecologia 111:1–11.

Cavaleri MA, Oberbauer SF, Ryan MG. 2006. Wood $CO_2$ efflux in a primary tropical rain forest. Global Change Biology 12:2442–2458.

Chambers JQ, Tribuzy ES, Toledo LC, Crispim BF, Higuchi N, dos Santos J, Araujo AC, Kruijt B, Nobre AD, Trumbore SE. 2004. Respiration from a tropical forest ecosystem: partitioning of sources and low carbon use efficiency. Ecological Applications 14:S72–S88.

Chave J, Andalo C, Brown S, Cairns MA, Chambers JQ, Eamus D, Folster H, Fromard F, Higuchi N, Kira T, et al. 2005. Tree allometry and improved estimation of carbon stocks and balance in tropical forests. Oecologia 145:87–99.

Chave J, Navarrete D, Almeida S, Alvarez E, Aragão LEOC, Bonal D, Chatelet P, Silva-Espejo JE, Goret JY, von Hildebrand P, et al. 2010. Regional and seasonal patterns of litterfall in tropical South America. Biogeosciences 7:43–55.

Delvaux B, Herbillon AJ, Vielvoye L. 1989. Characterization of a weathering sequence of soils derived from volcanic ash in Cameroon. Taxonomic, mineralogical and agronomic implications. Geoderma 45:375–388.

Domingues TF, Meir P, Feldpausch TR, Saiz G, Veenendaal EM, Schrodt F, Bird M, Djagbletey G, Hien F, Compaore H, et al. 2010. Co-limitation of photosynthetic capacity by nitrogen and phosphorus in West Africa woodlands. Plant Cell and Environment 33:959–980.

Doughty CE, Goulden ML. 2008. Seasonal patterns of tropical forest leaf area index and $CO_2$ exchange. Journal of Geophysical Research-Biogeosciences 113.

Doughty CE, Metcalfe DB, da Costa MC, de Oliveira AAR, Neto GFC, Silva JA, Aragão LEOC, Almeida SS, Quesada CA, Girardin CAJ, et al. 2014. Production, allocation and cycling of carbon in a forest on fertile terra preta soil in eastern Amazonia compared with a forest on adjacent infertile soil. Plant Ecology and Diversity 7(1–2):41–53.

Feldpausch TR, Banin L, Phillips OL, Baker TR, Lewis SL, Quesada CA, Affum-Baffoe K, Arets EJMM, Berry NJ, Bird M, et al. 2011. Height-diameter allometry of tropical forest trees. Biogeosciences 8:1081–1106.

Galbraith D, Malhi Y, Castanho ADA, Quesada CA, Doughty CE, Peh KS-H, Affum-Baffoe K, Lewis SL, Sonké B, Phillips OL, et al. 2013. The residence time of woody biomass in tropical forests, Plant Ecology and Diversity 6:139–157.

Gentry AH. 1988. Changes in plant community diversity and floristic composition on environmental and geographical gradients Annals of Missouri Botanical Garden 75:1–34.

Girardin CAJ, Aragão LEOC, Malhi Y, Huaraca Huasco W, Metcalfe DB, Durand L, Mamani M, Silva-Espejo JE, Whittaker RJ. 2013. Fine root dynamics along an elevational gradient in tropical Amazonian and Andean forests. Global Biogeochemical Cycles 27:252–264.

Girardin CAJ, Malhi Y, Aragão LEOC, Mamani M, Huaraca Huasco W, Durand L, Feeley KJ, Rapp J, Silva-Espejo JE, Silman M, et al. 2010. Net primary productivity allocation and cycling of carbon along a tropical forest elevational transect in the Peruvian Andes. Global Change Biology 16(12): 3176–3192.

Higgins MA, Ruokolainen K, Tuomisto H, Llerena N, Cardenas G, Phillips OL, Vásquez R, Räsänen M. 2011. Geological control of floristic composition in Amazonian forests. Journal of Biogeography 38:2136–2149.

Hoorn C, Wesselingh FP, ter Steege H, Bermudez MA, Mora A, Sevink J, Sanmartín I, Sanchez-Meseguer A, Anderson CL, Figueiredo JP, et al. 2010. Amazonia through time: Andean uplift, climate change, landscape evolution, and biodiversity. Science 330:927–931.

Hughes IG, Hase TPA. 2010. Measurements and their uncertainties: a practical guide to modern error analysis. Oxford (UK): OUP.

IUSS Working Group WRB. 2006. WRB: world reference base for soil resources 2006. A framework for international classification, correlation and communication. World Soil Resources Report 103, Rome: FAO.

Jackson RB, Canadell J, Ehleringer JR, Mooney HA, Sala OE, Schulze ED. A global analysis of root distributions for terrestrial biomes. Oecologia 108:389–411.

Kira T. 1978. Community architecture and organic matter dynamics in tropical rainforests of Southeast Asia with special reference to Pasoh Forest, West Malaysia. In: Tomlinson PB, Zimmerman MH, editors. Tropical Trees as Living Systems. Cambridge (UK): Cambridge University Press. p. 561–590.

Levy PE, Jarvis PG. 1998. Stem $CO_2$ fluxes in two Sahelian shrub species (Guiera senegalensis and Combretum micranthum). Functional Ecology 12:107–116.

Levy PE, Meir P, Allen SJ, Jarvis PG. 1999. The effect of aqueous transport of $CO_2$ in xylem sap on gas exchange in woody plants. Tree Physiology 19:53–59.

Lewis SL, Brando PM, Phillips OL, van der Heijden GMF, Nepstad D. 2011. The 2010 Amazon drought. Science 331:554–555.

Lloyd J, Patiño S, Paiva RQ, Nardoto GB, Quesada CA, Santos AJB, Baker TR, Brand WA, Hilke I, Gielmann H, et al. 2010. Optimisation of photosynthetic carbon gain and within-canopy gradients of associated foliar traits for Amazon forest trees. Biogeosciences 7:1833–1859.

Malhi Y. 2012. The productivity, metabolism and carbon carbon cycle of tropical forest vegetation. Journal of Ecology 100:65–75.

Malhi Y, Aragão LEOC, Metcalfe DB, Paiva R, Quesada CA, Almeida S, Anderson L, Brando P, Chambers JQ, da Costa ACL, et al. 2009. Comprehensive assessment of carbon productivity, allocation and storage in three Amazonian forests. Global Change Biology 15:1255–1274.

Malhi Y, Baker TR, Phillips OL, Almeida S, Alvarez E, Arroyo L, Chave J, Czimczik CI, di Fiore A, Higuchi N, et al. 2004. The above-ground coarse wood productivity of 104 Neotropical forest plots. Global Change Biology 10:563–591.

Malhi Y, Doughty C, Galbraith D. 2011. The allocation of ecosystem net primary productivity in tropical forests. Philosophical Transactions of the Royal Society B-Biological Sciences 366:3225–3245.

Malhi Y, Phillips OL, Lloyd J, Baker T, Wright J, Almeida S, Arroyo L, Frederiksen T, Grace J, Higuchi N, et al. 2002. An international network to monitor the structure, composition and dynamics of Amazonian forests (RAINFOR). Journal of Vegetation Science 13:439–450.

Malhi Y, Wood D, Baker TR, Wright J, Phillips OL, Cochrane T, Meir P, Chave J, Almeida S, Arroyo L, et al. 2006. The regional variation of aboveground live biomass in old-growth Amazonian forests. Global Change Biology 12:1107–1138.

Marthews TR, Malhi Y, Girardin CAJ, Silva-Espejo SE, Aragão LEOC, Metcalfe DB, Rapp JM, Mercado LM, Fisher RA, Galbraith DR, et al. 2012. Simulating forest productivity along a neotropical elevational transect: temperature variation and carbon use efficiency. Global Change Biology 9:2882–2898.

Martin AR, Thomas SC. 2011. A reassessment of carbon content in tropical trees. PLOS One 6.

Meir P, Grace J, Miranda AC. 2000. Photographic method to measure the vertical distribution of leaf area density in forests. Agricultural and Forest Meteorology 102:105–111.

Mercado LM, Patiño S, Domingues TF, Fyllas NM, Weedon GP, Sitch S, Quesada CA, Phillips OL, Aragão LEOC, Malhi Y. 2011. Variations in Amazon forest productivity correlated with foliar nutrients and modelled rates of photosynthetic carbon supply. Philosophical Transactions of the Royal Society B 366:3316–3329.

Metcalfe DB, Williams M, Aragao LEOC, da Costa ACL, de Almeida SS, Braga AP, Goncalves PHL, de Athaydes Silva Junior J, Malhi Y, Meir P. 2007. A method for extracting plant roots from soil which facilitates rapid sample processing without compromising measurement accuracy. New Phytologist 174:697–703.

Metcalfe DB, Meir P, Aragão LEOC, Lobo-do-Vale R, Galbraith D, Fisher RA, Chaves MM, Maroco JP, da Costa ACL, de Almeida SS, et al. 2010. Shifts in plant respiration and carbon use efficiency at a large-scale drought experiment in the eastern Amazon. New Phytologist 187:608–621.

Odum HT, Pigeon RF. 1970. A tropical rain forest. Washington (DC): Office of Information Services, US Atomic Energy Commission.

Phillips OL 1993. The potential for harvesting fruits in tropical rainforests: new data from Amazonian Peru. Biodiversity and Conservation 2:18–38.

Phillips OL, Aragão LE, Lewis SL, Fisher JB, Lloyd J, López-González G, Malhi Y, Monteagudo A, Peacock J, Quesada CA, et al. 2009. Drought sensitivity of the Amazon rainforest. Science 323:1344–1347.

Phillips OL, Baker TR, Arroyo L, Higuchi N, Killeen TJ, Laurance WF, Lewis SL, Lloyd J, Malhi Y, Monteagudo A, et al. 2004. Pattern and process in Amazon tree turnover, 1976–2001. Philosophical Transactions of the Royal Society of London Series B-Biological Sciences 359:381–407.

Phillips OL, Malhi Y, Higuchi N, Laurance WF, Nunez PV, Vasquez RM, Laurance SG, Ferreira LV, Stern M, Brown S, et al. 1998. Changes in the carbon balance of tropical forests: evidence from long-term plots. Science 282:439–442.

Quesada CA, Lloyd J, Schwarz M, Patiño S, Baker TR, Czimczik C, Fyllas NM, Martinelli L, Nardoto GB, Schmerler J, et al. 2010. Variations in chemical and physical properties of Amazon forest soils in relation to their genesis. Biogeosciences 7:1515–1541.

Quesada CA, Lloyd J, Anderson LO, Fyllas NM, Schwarz M, Czimczik CI. 2011. Soils of Amazonia with particular reference to the RAINFOR sites. Biogeosciences 8:1415–1440.

Quesada CA, Phillips OL, Schwarz M, Czimczik C, Baker TR, Patiño S, Fyllas NM, Hodnett MG, Herrera R, Almeida S, et al. 2012. Basin-wide variations in Amazon forest structure and function are mediated by both soils and climate. Biogeosciences 9:2203–2246.

Robertson AL, Malhi Y, Farfan-Amezquita F, Aragão LEOC, Silva Espejo JE, Robertson MA. 2010. Stem respiration in tropical forests along an elevation gradient in the Amazon and Andes. Global Change Biology 16:3193–3204.

Tan ZH, Zhang YP, Yu GR, Sha LQ, Tang JW, Deng XB, Song QH. 2010. Carbon balance of a primary tropical seasonal rain forest. Journal of Geophysical Research Atmospheres 115:D00H26.

ter Steege H, Pitman NCA, Phillips OL, Chave J, Sabatier D, Duque A, Molino J, Prévost M, Spichiger R, Castellanos H, et al. 2006. Continental-scale patterns of canopy tree composition and function across Amazonia. Nature 443:444–447.

Teskey RO, McGuire MA. 2002. Carbon dioxide transport in xylem causes overestimation of rates of respiration in trees. Plant, Cell and Environment 25:1571–1577.

Vicca S, Luyssaert S, Penuelas, Campioli JM, Chapin III FS, Ciais P, Heinemeyer A, Hogberg P, Kutsch WL, Law BE, et al. 2012. Fertile forests produce biomass more efficiently. Ecology Letters 15:520–526.

Wurth MKR, Pelaez-Riedl S, Wright SJ, Korner C. 2005. Non-structural carbohydrate pools in a tropical forest. Oecologia 143:11–34.

Zimmermann M, Meir P, Bird MI, Malhi Y, Ccahuana AJQ. 2010. Temporal variation and climate dependence of soil respiration and its components along a 3000 m altitudinal tropical forest gradient. Global Biogeochemical Cycles 24:GB4012.

Zimmermann M, Meir P, Bird MI, Malhi Y, Ccahuana AJ. 2009. Climate dependence of heterotrophic soil respiration from a soil-translocation experiment along a 3000 m tropical forest altitudinal gradient. European Journal of Soil Science doi: 10.1111/j.1365-2389.2009.01175.x.